Reviews and syntheses: Eddy covariance-based evapotranspiration partitioning

Emma G. Cochran[1], Claudia Wagner-Riddle[2], Elke Eichelmann[1]

[1]School of Biology and Environmental Science, University College Dublin, Belfield, Dublin 4, Ireland
[2]School of Environmental Sciences, University of Guelph, Guelph, Ontario, Canada

Correspondence to: Emma G. Cochran (cochranemma17@gmail.com)

Abstract. The task of reliably partitioning evapotranspiration (ET) is imperative so that we can better understand how individual components of the terrestrial water flux are contributing to the global hydrological cycle and changing under a warming climate. By constraining how evaporation (E) and transpiration (T) separately adapt to increased global temperatures, we can make more accurate predictions in land surface models, further our understanding of plant water use, and better manage our limited water resources. Eddy covariance (EC) is a globally used technique that measures net biosphere-atmosphere fluxes, including ET, and if reliably partitioned, presents a promising way to constrain E and T values and trends across ecosystems. Several EC-based ET partitioning methods exist, and there is a need for an updated comprehensive guide to the available approaches. This systematic literature review was conducted with the objectives of 1) identifying EC-based ET partitioning methods and categorizing them based on underlying ecosystem assumptions, 2) determining the main advantages and disadvantages of each method dependent on their assumptions and data requirements, and 3) evaluating how broadly these methods have been applied based on geographic location and ecosystem type. The review identified 11 independent partitioning methods applied across 129 studies. Methods using assumptions of underlying water use efficiency (uWUE) and ecosystem conductance all use the relationship between ET and gross primary production with vapor pressure deficit (VPD) to estimate the transpiration ratio (T/ET). Additionally, two machine learning based methods, one method assuming a linear relationship between ET and gross ecosystem photosynthesis, and four methods using high frequency EC data to estimate T/ET were identified. The uWUE methods, while the most frequently used partitioning approach, consistently predicted the lowest T/ET estimates when compared to both other EC and many non-EC based partitioning methods. The machine learning methods predicted the highest T/ET values compared to other EC-based methods which agreed well with values estimated with independent methods. Savannas and evergreen broadleaf forests had the highest T/ET of all ecosystem types while deserts and wetlands had the lowest. Leaf area index and soil water content were found to be the most important drivers of T/ET values and trends with VPD and air temperature also displaying significant effects. Of the global studies identified in this review, an average annual T/ET value of 0.573 ± 0.10 was found, a value that falls within the range of other studies using isotopic partitioning, remote sensing methods, and global estimates from various ecosystem models. More testing, specifically increased paired analyses of two or more EC-based ET partitioning methods on the same dataset and more validations against

independent observations, are needed in order to fully understand the applicability of each method, their differences, and to better constrain global T/ET dynamics.

1 Introduction

Evapotranspiration (ET) is the combined water flux of terrestrial ecosystems whereby 65,000 – 76,000 km^3 of water leaves land surfaces to the atmosphere annually (Dorigo et al., 2021; Jung et al., 2019; Oki & Kanae, 2006). While global ET trends will continue to change under the warming climate, land surface models (LSM) have not converged on a predicted trend with some models indicating an increase in global ET due to increased temperatures (Brutsaert, 2017; Zeng et al., 2018) and other models indicating a decrease due to decreased water supply (Gedney et al., 2006; Jung et al., 2010). The importance of properly constraining the water flux in LSMs is paramount so that we can further our understanding of the terrestrial water cycle and better manage water resources under a changing climate (Dolman et al., 2014; Fisher et al., 2017; Stoy et al., 2019). However, to reliably model and predict ET, we must understand its two primary components: evaporation (E) and transpiration (T).

Evaporation is a physical process by which water is lost from non-stomatal surfaces. This is most often from soil surfaces (bare soil evaporation) but can extend to a wet canopy (including leaves and moist ground surfaces) following a precipitation event (hereafter interception evaporation will refer to any E from wet surfaces directly following rain) or include snow sublimation in high-elevation sites. Water availability and vapor pressure deficit (VPD) are major drivers of E where the magnitude of E increases when atmospheric water demand and the surface soil water content are high (Kool et al., 2014; Scott & Biederman, 2017). Transpiration is water lost through stomata during carbon assimilation, linking the carbon and water fluxes from vascular plants (Katul et al., 2012; Kool et al., 2014; Li et al., 2019; Zhou et al., 2016). T is the other major component of ET, but has large uncertainties on a global scale, accounting for anywhere from 35-90% of the annual water flux from land surfaces (Coenders-Gerritis et al., 2014; Good et al., 2015; Jasechko et al., 2013; Schlesinger & Jasechko, 2014; Wang et al., 2014). T is largely dependent on leaf physiology and is difficult to estimate in heterogenous ecosystems (Nelson et al., 2020; Reich et al., 2024). Like E, T is also dependent on soil water availability and VPD (Beer et al., 2009; Grossiord et al., 2020; López et al., 2021b). T is predicted to increase with rising global VPD, leading to a decrease in plant water use efficiency (López et al., 2021b; Novick et al., 2016; Yuan et al., 2019) although this response is highly variable depending on plant species and environmental conditions (Grossiord et al., 2020). Because T is a major component of the terrestrial water flux, its shifts in magnitude due to climate change will have repercussions for the rest of the global water cycle (Berkelhammer et al., 2016; Gerken et al., 2018).

While both T and E have similar and even overlapping drivers, the rates at which they respond to these drivers are unequal in magnitude (Scott and Biederman, 2017). For example, the timescales on which E and T operate differ significantly, another factor impacting the hydrological cycle (Scott et al., 2006; Scott and Biederman, 2017). Rates of E will increase in response to any precipitation event that results in wet surfaces. On the other hand, T will only respond to rainfall when enough water has entered the root zone to allow for plant water uptake, a response that can lag up to 10 days after the precipitation event (Feldman et al., 2018; Kurc and Small, 2007; Scott et al., 2006). Beyond these direct effects, precipitation also indirectly modulates T and E by influencing their response to other environmental drivers (da Rocha et al., 2022). For example, rainfall promotes plant growth and increases leaf area index (LAI), which subsequently enhances T (Lowry et al., 2021; Wagle et al., 2020). Conversely, drought stress can cause quick increases in E (through elevated temperatures and vapor pressure deficits) but if prolonged, decreases in T (through LAI decline and reduced plant water uptake), creating opposing responses in the two fluxes (Nie et al., 2021; Restrepo-Coupe et al., 2023). The recovery from drought also illustrates their divergent timescales: E rebounds immediately upon rewetting, but T may remain suppressed for months or even a year as LAI recovers from stress, a response especially true in tall canopies with high correlations between T and LAI (Restrepo-Coupe et al., 2023; Sun et al., 2020). As such, perhaps the biggest difference in the drivers of T and E is that T is significantly affected by vegetation characteristics and plant water dynamics, while E is only dependent on environmental conditions (Wang et al., 2014; Zhou et al., 2016). This makes T an active, biotic process regulated by stomatal conductance, while E remains a passive, abiotic process. The differentiation of the biotic and abiotic components of ET allows for the study of how the water cycle is impacted by changes in vegetation (Cao et al., 2010; Scott and Biederman, 2017; Wilcox et al., 2012). By quantifying the relative contributions of T and E, we can also study the influences of changing climatic and biological conditions on the spatial and temporal variability of ET (Gan and Liu, 2020; Reich et al., 2024).

Eddy covariance (EC) is a technique used to measure ecosystem gas and heat exchange within the atmospheric boundary layer, including ET (Baldocchi, 2020). EC systems take above-canopy, high frequency (usually 10 Hz) measurements of water vapor mixing ratio and three-dimensional wind velocity in order to continuously measure ET, which is then aggregated to half-hour fluxes to study how an ecosystem's ET is continuously changing in response to environmental factors (Baldocchi, 2020; Kool et al., 2014; Stoy et al., 2019). Methods have been developed to then partition measured ET into its relative components rather than measuring each part individually. This allows for long-term studies of an ecosystem's T and E dynamics from easily available data in global biomes (Cao et al., 2022; Maes et al., 2020; Nelson et al., 2020; Xue et al., 2023). On the other hand, direct measurements of T or E by means of isotopic, sap-flux, or soil evaporation methods are time, money, and labor intensive and are associated with significant uncertainties when upscaling to the ecosystem level (Cammalleri et al., 2013; Griffis, 2013; Kool et al., 2014; Li et al., 2019; Oishi et al., 2008; Poyatos et al., 2016; Stoy et al., 2019; Wilson et al., 2001). Modeling methods often require complex parameterization and require validation data not easily accessible (Fatichi and Pappas, 2017; Kool et al., 2014; Sun et al., 2018). As such, using EC-measured ET data with an appropriate partitioning method positions researchers to study E and T dynamics even without extensive field campaigns. Previous reviews focused on deriving E and T through model-based approaches (i.e., Shuttleworth-Wallace, FAO-Dual KC, TSEB, and Priestley-Taylor) as well as non-EC data-based methods (i.e., solar induced fluorescence-based, carbonyl sulfide flux-based, and isotope-based) exist (Kool et al., 2014; Stoy et al., 2019), however, there is a need for an updated, comprehensive review of EC-based partitioning methods.

FLUXNET, a collaboration of EC networks, provides open-source, public micrometeorological data from hundreds of ecosystems under various climates which can be used to create spatial maps of global carbon and water fluxes (Baldocchi, 2020; Pastorello et al., 2020; Williams et al., 2009). Because of this, FLUXNET data is often used as ground truth to validate and parameterize remote sensing data products and LSMs. Therefore, partitioned E and T data derived from EC ecosystem water data, would improve LSMs' prediction capabilities (Bonan et al., 2011, 2012; Chaney et al., 2016; Friend et al., 2007; Kool et al., 2014; Nogueira et al., 2021; Reich et al., 2024; Stapleton et al., 2022; Stoy et al., 2019; Williams et al., 2009). Additionally, the continuous, high-frequency measurements allow for flux analyses ranging from 30 min intervals to interannual trends, giving researchers key insights into how ecosystem water pathways behave and evolve over time in response to a changing climate (Baldocchi, 2003, 2020; Eichelmann et al., 2022).

Previous work in partitioning the terrestrial ecosystem carbon flux from EC-measured net ecosystem exchange (NEE) into gross primary production (GPP) and ecosystem respiration has led to significant improvements in understanding the interannual variability of NEE across ecosystems (Lasslop et al., 2010; Reichstein et al., 2005). This has furthered our understanding of global and regional carbon fluxes as well as aided in the study of the role of vegetation as a vital carbon sink (Chatterjee et al., 2020; Stoy et al., 2006). The ability to partition the terrestrial ecosystem water flux from FLUXNET data will have implications of a similar magnitude. Various methods exist to partition EC-measured ET and there is a need to create a comprehensive guide to the available approaches.

Here we reviewed EC-based ET partitioning methods using data routinely collected at flux towers to answer three questions:

1. What EC-based ET partitioning methods exist and on which ecosystem assumptions are they based?
2. Based on ecosystem assumptions and data availability, what are the main advantages and disadvantages of each method?
3. What is the breadth (geographic location and ecosystem type) of application of each method?

This review, in line with much of current work, presents the transpiration ratio (T/ET) to evaluate partitioning results and includes methods that could be applied on any FLUXNET dataset. Hereafter, a method application would be any instance of partitioning applied to a flux dataset while method testing would refer to instances where partitioning estimates are compared against ground truth data or an independent, non-EC-based partitioning method.

2 Methods

A systematic literature review was conducted of ET partitioning methods including studies that reported T and E with ET data or T/ET ratios calculated using data routinely collected from eddy covariance sites. EC-based ET partitioning methods were categorized by underlying principles. Several sub-methods were identified as slight adjustments to previously established methods and are also discussed. The search was conducted using the Web of Science Core Collection (WoSCC), Scopus, and University College Dublin's OneSearch database, a public online database search tool that encompasses hundreds of journals across disciplines. The following key words were used: "evapotranspiration partitioning eddy covariance", "eddy covariance latent heat partitioning", "flux variance similarity evapotranspiration", "eddy covariance transpiration evaporation ratio", and "eddy covariance evapotranspiration components". Additionally, papers that had cited an established EC-based partitioning method were identified using WoSCC and screened for eligibility. Only peer reviewed studies published in English were included, excluding theses and conference papers. The databases were last searched on May 22nd, 2026.

Partitioning methods that use EC data combined with data from other sources (often LAI, remote sensing products, isotopes, or LSMs) were excluded. Data reported in either numerical or graphical formats were included. If the values or trends of T/ET could not be determined from the reported data (often in the case where correlation coefficients or statistical results were reported in terms of how one partitioning method compared to another method), the study was excluded.

Above- and below-canopy concurrent EC measurements can be used to partition ET in forests and savannas by assuming the below-canopy system measures only soil E which is then subtracted from the above-canopy ET measurements to find overstory T (Ma et al., 2020; Paul-Limoges et al., 2020; Sulman et al., 2016; Wilson et al., 2001). However, this method requires dual EC systems across a vertical profile and therefore was excluded from the identified methods as below canopy measurements are not routinely collected. Additionally, some of the underlying assumptions of EC theory, such as low wind speeds, constant turbulence, and heterogeneity, are not met under the canopy of many ecosystem types, again limiting the applicability of this method (Misson et al., 2007).

The resulting studies were then screened by one reviewer with no automation tools. If available, data pertaining to T or E with ET values and/or trends, T/ET values and/or trends, the temporal scale on which the partitioning method was applied, the flux site location (and site I.D. when provided), and plant functional type (PFT) were extracted. If results were provided in both graphical and numerical contexts, the numerical data were included. Supplementary documents were searched in conjunction with the main text of the screened studies and eligible data were extracted in the same way. A total of 1432 papers were identified in the original search, however, only 129 (=N_S) papers were included in the final review (Fig. 1). The number of records (N_R) or datasets reported within a study was also recorded. For instance, if a study conducted analyses in 3 different ecosystem types and reported separate T/ET values for each, N_S would equal 1 while N_R would equal 3.

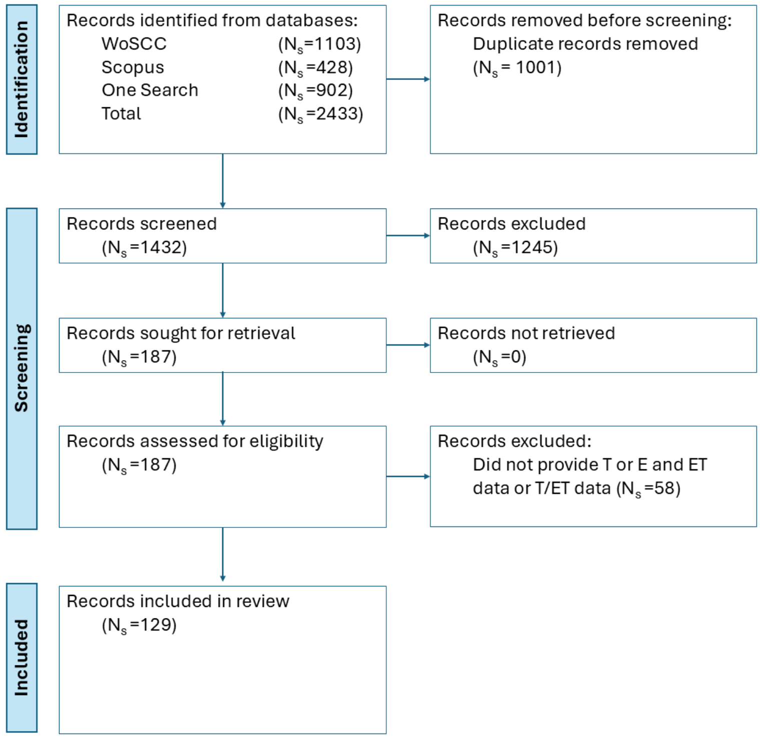

Figure 1: PRISMA 2020 flow diagram for systematic reviews (Page et al., 2021) showing for the review: the databases searched, the number of studies found (N_S), and the number of studies included in the final review. Reports excluded includes any papers that do not fit the required criteria of inclusion, while reports not retrieved would indicate any papers inaccessible online.

3 Results

3.1 ET partitioning methods, their assumptions, advantages, and disadvantages

Eleven independent partitioning methods were identified, each built from a range of ecosystem assumptions. Methods were deemed as independent if the theory on which they are based or process of T/ET calculation are substantially different to all other methods. Methods based on the concept of underlying water use efficiency (uWUE) were compared to ecosystem conductance-based methods, machine learning methods, methods requiring high frequency data, and linear regression-based methods (Table 1).

Table 1: Summary table of EC-based ET partitioning methods, their data requirements, theory, and main advantages/disadvantages. Independent methods have their own abbreviation while sub-methods are denoted with a ‘b’ and

the abbreviation of the method on which they are based. GPP: gross primary production, VPD: vapor pressure deficit, RH: relative humidity, ET: evapotranspiration, uWUE: underlying water use efficiency, LE: latent heat flux, H: sensible heat flux, G: ground heat flux, T_A: air temperature, T_S: soil temperature, C_A: ambient CO_2 mixing ratio, PA: air pressure, u*: friction velocity, WS: wind speed, ↓K: incoming shortwave radiation, ↑K: outgoing shortwave radiation, ↓L: incoming longwave radiation, ↑L: outgoing longwave radiation, $↓K_{POT}$: potential incoming shortwave radiation, Z: altitude, PAR: photosynthetically active radiation (from the PPFD_IN variable in FLUXNET datasets), P: precipitation, c: CO_2 concentration, q: H_2O concentration, u: wind speed from the predominate direction, v: cross-stream wind speed, w: vertical wind speed

Method Type	Method	Data Required	Basic Theory	Advantages	Disadvantages	Source
uWUE	ZH16	GPP, VPD, ET	An ecosystem has a potential uWUE (when ET=T) and an actual uWUE which when combined are proportional to T/ET	T/ET estimates from daily to annual timescales, easy implementation	Reliance on GPP estimates, methods assumptions do not hold in heterogenous ecosystems, wetlands, or under low VPD conditions	(Zhou et al., 2016)
	BH16	GPP, VPD, ET	Similar to ZH16, except potential uWUE is determined using binned GPP values	Does not exclude rainy periods, easy implementation	Same as ZH16	(Berkelhammer et al., 2016)
Stomatal conductance	LI19	GPP, VPD, ET, soil moisture	Parameter optimization to separate surface conductance into its soil and canopy components, which are proportional to T/ET	Takes into account vegetation type, does not assume periods where ET=T	Reliance on GPP estimates, excludes rainy and wet periods, method assumptions do not hold in heterogenous ecosystems or drylands	(Li et al., 2019)
	PP18	GPP, VPD, LE, H, T_A, C_A, P_A, u*, WS, ↓K, Z, PAR	Big-leaf canopy model used to estimate canopy conductance responses to	Does not assume periods where ET=T	Same as LI19, often fails to produce physically-	(Perez-Priego et al., 2018)

			changing environmental conditions		realistic T estimates	
Machine learning	TEA18	GPP, VPD, ET, $\downarrow K$, $\downarrow K_{POT}$ T_A, P, WS	Uses a Random Forest regressor to estimate WUE when ET=T to be used with GPP to estimate half-hour T	Captures half hourly patterns of T from minimal data requirements, low computational power requirements	Excludes rainy and wet periods, method assumptions not held in ecosystems with significant E contributions	(Nelson et al., 2018)
	EE22	VPD, H, T_A, u*	Uses a neural network to partition daytime ET fluxes assuming nighttime ET=E	Does not rely on periods when T=ET, does not use GPP estimates	Requires site-specific knowledge for feature selection*, method assumptions not held in ecosystems with nocturnal transpiration	(Eichelmann et al., 2022)
High frequency	SK10	High frequency c, q, u, v, w	Stomatal (T) and non-stomatal (E) processes independently adhere to flux variance similarity	Open source through Fluxpart, customization in WUE calculation	Requires high frequency data, assumptions not met in heterogenous canopies, often fails to produce physically realistic T estimates	(Scanlon & Kustas, 2010; Scanlon & Sahu, 2008)
	TH08	High frequency c, q, u, v, w	Similar to SK10 but identifies updrafts where c and q are equal to E	Created for ecosystems with tall, low-density canopies but has been shown to work well in dense canopies**	Requires high frequency data, heavy computational power required	(Thomas et al., 2008)
	TH08b	High frequency c, q, u, v, w	Conditional eddy accumulation method, similar to TH08 but includes downdrafts	Does not require a priori knowledge of WUE	Same as TH08	(Zahn et al., 2024)

	ZN22	High frequency c, q, u, v, w	Conditional eddy covariance method, defines conditional covariances where w and q are proportional to E and T	Does not require a priori knowledge of WUE	Requires high frequency data, heavy computational resources required	(Zahn et al., 2022)
	ZN22b	High frequency c, q, u, v, w, WUE	Same as ZN22 but with the addition of WUE if known to better constrain the carbon flux	Simpler than SK10, allowing for easier implementation	Same as ZN22	(Zahn et al., 2024)
	RB26	High frequency c, q, u, v, w, T estimates from TH08b, soil moisture, T_A, T_S, ↓K, ↑K, ↓L, ↑L, PAR, RH, VPD, WS, u*, G, P	Uses a knowledge-guided neural network trained on physical parameters and transpiration estimates from TH08b to estimate T, direct E, and interception E	Publicly available code, better constrains intercepted E compared to other high frequency methods	Heavy data and computational requirements. The model trains on estimates from another method, potentially amplifying any uncertainties from TH08b	(Ranjbar et al., 2026)
Linear regression	SB17	GPP, ET	T is related to GPP on an interannual basis and can be solved for by using a linear regression on monthly timescales	No assumption that ET=T, easy implementation	Ideal datasets of 5-7 years of length (minimum 3 years) limit site applicability, suppresses rainy periods	(Scott & Biederman, 2017)
	SB17b	GPP, ET	Built off of SB17 to estimate weekly WUE and subsequent weekly T	Daily to weekly T estimates improved from monthly estimates from SB17	Not well suited for heterogenous ecosystems	(Reich et al., 2024)

*This was adjusted for in Stapleton et al., 2022

**From Klosterhalfen et al. (2019a)

3.1.1 Underlying water use efficiency

Zhou et al. (2016) established a method (hereafter, ZH16) based on underlying water use efficiency (uWUE) to partition ET based on half-hourly flux data. This method assumes that at sub-daily time scales, periods occur when soil and interception evaporation are negligible and T/ET approaches 1, often periods experiencing limited water availability, maintained vegetation cover, and depleted subsurface soil moisture following dry-down periods. These conditions are then used to define the potential uWUE ($uWUE_p$), a value assumed to be constant over long time periods and calculated using a 95th percentile regression on the assumed linear relationship between ET and GPP x $VPD^{0.5}$. This relationship relies on stomatal optimality assumptions based on earlier work (Cowan & Farquhar, 1977; Farquhar & Sharkey, 1982; Zhou et al., 2014) which is also used to calculate the actual uWUE ($uWUE_a$) with a regular linear regression. $uWUE_p$ is then related to T while the $uWUE_a$ is related to ET. $uWUE_p$ is estimated just once using all data available for the site while $uWUE_a$ is estimated over the time period during which T/ET is being predicted.

$$uWUE_a = \frac{GPP*VPD^{0.5}}{ET}, \tag{1}$$

$$uWUE_p = \frac{GPP*VPD^{0.5}}{T}, \tag{2}$$

Subsequently, T/ET is estimated using the ratio of actual to potential uWUE:

$$\frac{T}{ET} = \frac{uWUE_a}{uWUE_p}, \tag{3}$$

The uWUE assumptions make this method widely accessible to any flux site since only half-hourly flux data of GPP, VPD, and ET are needed in order to estimate T/ET from daily to annual timescales. The heavy reliance on GPP estimates from EC measurements mean that any uncertainties in GPP are amplified when predicting T using this method and the assumption of a constant $uWUE_p$ is violated in sites with a wide variety of vegetation types as spatial variations in plant heights and structures result in subsequent seasonal variations in CO_2 concentrations (Hu & Lei, 2021; Nelson et al., 2020; Reich et al., 2024; Stoy et al., 2019; Zhou et al., 2016). Additionally, the assumption that T=ET does not hold true throughout the day in ecosystems with sparse vegetation or where evaporation is never negligible such as in wetland ecosystems (Eichelmann et al., 2022; Li et al., 2019; Reich et al., 2024; Zhou et al., 2016). Interception evaporation is also ignored in this method as days with and immediately following rainfall are filtered out before the partitioning begins.

Berkelhammer et al. (2016) follows a similar procedure with similar assumptions (BH16), however, after plotting ET against GPP x $VPD^{0.5}$, the GPP values are binned, and the minimum ET values are found for each bin. These minimum ET values are then thought to represent times when T/ET = 1 and the rest of the ET values are used to estimate T:

$$\frac{T}{ET} = \frac{min_{GPP}\,\|ET\|}{ET_{flux}}, \tag{4}$$

The threshold for which to define the minimum ET values varies by site but is dependent on LAI, known biases of instruments, and the sites specific biome. However, because this method keeps the assumption from the ZH16 method whereby T/ET approaches 1 at sub-daily timescales, the same limitations apply with regards to application to ecosystems where E consistently and significantly contributes to ET. Additionally, assuming there is a linear relationship between ET and GPP x $VPD^{0.5}$ assumes a constant direct response of stomatal conductance to VPD which is not met under low VPD conditions (Addington et al., 2004; Day, 2000; Ocheltree et al., 2014). However, rainy days are not filtered out from the dataset, so while interception evaporation is not separately estimated, it is included within E estimates.

3.1.2 Stomatal conductance

Li et al. (2019) partitions ET using previously established assumptions of canopy and aerodynamic resistances (Monteith, 1965; Penman, 1948; Shuttleworth and Wallace, 1985). This method (LI19) estimates ecosystem conductances to sidestep the assumption that T/ET approaches 1. Here, a parameter optimization is added to an ecosystem conductance (G_s) model (Lin et al., 2018) to separate surface conductances. This method excludes rainy periods and times when interception E contributes to ET so that G_s can be split into soil (G_{soil}) and canopy (G_{veg}) conductances, or soil evaporation and canopy transpiration, respectively, and G_s is calculated using EC data in the inverted Penman-Monteith equation using:

$$G_s = G_{soil} + G_{veg} = G_0 + G_1 \frac{GPP}{VPD_l^m}, \tag{5}$$

G_s and GPP values are binned according to soil moisture, and a non-linear regression is run on Equation 5 to fit the ecosystem-level parameters: G_0, G_1, and m. G_{soil} and G_{veg} can then be calculated in each soil moisture bin and ET is partitioned using assumptions similar to Shuttleworth & Wallace (1985):

$$\frac{T}{ET} = \frac{G_{veg}}{G_s}, \tag{6}$$

$$\frac{E}{ET} = \frac{G_{soil}}{G_s}, \tag{7}$$

Parameterizing m allows VPD's dependence on GPP to vary depending on vegetation type, a strength compared to methods using the assumption from Zhou et al. (2014) where a constant m of 0.5 assumes an optimal linear relationship between ET and GPP x $VPD^{0.5}$ regardless of ecosystem type. However, LI19 was founded on the assumption that G_s is the sum of soil and canopy conductances, which is only true assuming there is a constant temperature throughout the canopy and soil surface, and not held in heterogeneous ecosystems (Li et al., 2019). Additionally, the exclusion of all rainy data has greater limitations in wet ecosystems where interception E is rarely negligible, and the necessity of soil moisture data limits its applicability to all flux sites (Hu and Lei, 2021; Li et al., 2019).

Perez-Priego et al. (2018) also partitions ET using model predicted ecosystem conductances (PP18). Starting with the assumption of optimality theory on a big-leaf canopy (Cowan & Farquhar, 1977; Wang et al., 2017), the patterns of canopy-scale internal leaf-to-ambient CO_2 (χ) are modelled based on temperature, elevation, and VPD. Optimality theory ensures that the model parameters are estimated assuming the big-leaf canopy model minimizes T while maximizing photosynthesis. Then using GPP in conjunction with χ, as well as the ambient CO_2 mixing ratio and molar air density, ecosystem stomatal conductance (g_c) is modelled. T is then estimated by:

$$T = 1.6 \cdot g_c \cdot VPD, \tag{8}$$

Where 1.6 is the diffusivity factor for CO_2 and water vapor. PP18 avoids the assumption that ecosystem ET equals T however, upon application of PP18, Nelson et al. (2020) found that the model was not always able to converge to realistic T values, with 30% of predictions being unusable. The method also relies on GPP estimates and therefore will be impacted by the uncertainties and biases of those values (Eichelmann et al., 2022; Nelson et al., 2020; Zhou et al., 2016). Additionally, to optimize the PP18 model, rainy periods and times with interception evaporation must be ignored which may lead to an overestimation of WUE and in turn underestimation of T (Perez-Priego et al., 2018).

3.1.3 Machine learning methods

Recently, several approaches using machine learning have been established to partition ET. Nelson et al. (2018) introduced the Transpiration Estimation Algorithm (TEA18) which uses a Random Forest regressor (Breiman, 2001) and isolates periods when T/ET ≈ 1 to estimate ecosystem WUE. The model achieves this by calculating the conservative surface wetness index to determine periods likely to have wet surfaces and excluding them from the training dataset. In order to account for further instances of E in the training dataset, a 75th percentile of ecosystem WUE is then used to determine model output. This predicted WUE (WUE_{pred}) can then be used to calculate T on half hourly intervals:

$$T = \frac{GPP}{WUE_{pred}} , \tag{9}$$

TEA18 can be easily applied to EC sites as it only requires GPP, ET, and simple meteorological data as inputs. However, because the model trains on dry periods where it is assumed that T/ET approaches 1, the behavior of WUE on rainy days and periods with interception evaporation will not be well represented in the model output. This leads to an overestimation of E in the training dataset and subsequent underestimation of T for ecosystems with sparse vegetation and wetland sites (Hu and Lei, 2021; Nelson et al., 2018; Reich et al., 2024).

Alternatively, Eichelmann et al. (2022) established a partitioning method (EE22) using an artificial neural network (Bishop, 1995) that assumes negligible nighttime transpiration values so therefore:

$$ET_{night} \approx E , \tag{10}$$

Daytime E is then predicted using measured nighttime ET values, similar to established methods of partitioning NEE into GPP and respiration based on nighttime NEE values (Reichstein et al., 2005). While daytime drivers of E may differ from nighttime E, neural networks have been shown to capture non-linear relationships of biological data, even when extrapolated beyond the subsets used for model training (Papale and Valentini, 2003). This was supported in the method establishment study when the model performed well when validated against daytime data collected after flooding periods (Eichelmann et al., 2022). Because there are no underlying assumptions that T/ET approaches 1, it is easier to apply this method to ecosystems with large contributions of E. By focusing on nighttime E, the model training process accounts for nocturnal interception evaporation but may fail to properly constrain daytime interception evaporation in E estimates. This is one of the few partitioning approaches that does not rely on any assumptions of the relationship between CO_2 uptake and water loss through stomata, making it a stronger method for wetlands and other ecosystems where E is never negligible and circumventing the need for GPP values.

However, while avoiding the assumption of zero E values, this method defaults to an assumption of zero T values, which is not met in every ecosystem and must be verified at sites before implementation (Dawson et al., 2007; Di et al., 2019; López et al., 2021a; Siddiq & Cao, 2018; Wang et al., 2021; Zeppel et al., 2010). EE22 also requires site-specific knowledge for model feature selection, although this has been adjusted by Stapleton et al. (2022) who introduced a machine learning framework consisting of 8 algorithms to identify the highest performing model for ET partitioning. The framework uses the assumptions from EE22 to estimate daytime E from nighttime ET measurements but conducts recursive feature elimination before training the model, a more objective approach as opposed to manual feature selection.

3.1.4 High frequency data

Instead of using EC data processed at a half-hourly resolution, several methods exist to partition ET directly from the high frequency data. This data, commonly collected at 10 Hz (18,000 measurements per half hour), is not publicly available and must be requested from EC tower operators. The data size and storage requirements often introduce issues when analyzing multiple sites across multiple years, however, by keeping data representing individual air parcels, assumptions on their origin can be made as opposed to when using aggregated 30-min fluxes.

Scanlon & Kustas, 2010 (SK10) established a method using the assumptions of flux variance similarity (FVS; Scanlon & Kustas, 2010; Scanlon & Sahu, 2008). This method is based on the Monin-Obukhov similarity theory assuming that both stomatal and non-stomatal components of carbon (c) and water (q) fluxes independently adhere to FVS. The stomatal processes, both photosynthesis and transpiration are thought to have a q-c correlation of −1, with the non-stomatal process of respiration and evaporation degrading this perfect correlation. Scanlon and Sahu (2008) introduced the idea that the degree of this degradation can be used to infer the magnitude of the non-stomatal processes. Leaf-level WUE is the only additional information needed to establish the relationship between the stomatal and non-stomatal processes in the carbon flux and estimate the components of both q and c. However, if leaf-level measurements are not available, WUE can be estimated from flux measurements, the ratio of molecular diffusivities for carbon dioxide and water vapor, and constants representing established leaf-level relationships of gas exchange.

Because large-scale eddies can affect the assumptions on which the FVS theory is based, wavelet filtering is required to remove the low-frequency data from the time series. Additionally, SK10 is computationally heavy as it uses optimization to solve the correlation between photosynthesis and respiration as well as the variance of photosynthesis. Fortunately, Skaggs et al. (2018) building on Palatella et al. (2014), solved these two parameters using algebra, significantly reducing computational time. Skaggs et al. (2018) also established Fluxpart, a free, open-source Python 3 module that runs the SK10 partitioning method on high frequency data. Fluxpart makes SK10 significantly more accessible to researchers and subsequently increased the use of this partitioning method. However, the need for high-frequency datasets remains the largest obstacle for widescale application of SK10. Additionally, the assumption that WUE remains constant over a given time interval is not representative of sites with significant heterogeneous vegetation or in ecosystems with a well-developed understory (Eichelmann et al., 2022; Scanlon & Kustas, 2010; Zhou et al., 2016). The default leaf-level WUE estimation used in Fluxpart is:

$$WUE = \frac{\frac{1}{1.6} * (c_a - c_i)}{q_a - q_i} , \tag{11}$$

Where c_a (q_a) and c_i (q_i) are the ambient and intercellular concentrations of CO_2 (H_2O), respectively and 1.6 is the diffusivity factor for CO_2 and water vapor. There are several parametrization schemes to estimate c_i. Commonly, these assumptions are made: c_i is a constant value, c_i/c_a is a constant ratio, or c_i/c_a has a linear or square root relationship with VPD (Campbell and Norman, 1998; Katul et al., 2009; Kim et al., 2006; Morison and Gifford, 1983; Sinclair et al., 1984). Alternatively, WUE can be optimized using assumptions of the relationship between c, q, and VPD (Scanlon et al., 2019).

Like SK10, the Modified Relaxed Eddy Accumulation method (TH08) introduced by Thomas et al. (2008) built on earlier work by Businger & Oncley (1990) to assume that the turbulent transport of non-stomatal components of carbon and water fluxes are similar. This method uses multi-scalar octant analysis to identify conditions where the q and c fluxes are equal to the soil flux component, or evaporation. The first octant (O1) is defined when the vertical velocity (w'), c', and q' are all greater than 0 (where w', c', q' are fluctuations from concurrent measurements), and using data that fits these criteria, evaporation is estimated as:

$$E_{TH08} = \beta \sigma_w \frac{\Sigma_{i=1}^{N} I_H q'}{\Sigma_{i=1}^{N} I_{H,w+}} , \tag{12}$$

Where N is the number of samples in the time series, β is the ratio between the standard deviation of the vertical velocity (σ_w) and the mean vertical velocities in updrafts and downdrafts, and I_H and I_{H,w_+} are hyperbolic thresholds. Because O1 is defined when w' > 0, the TH08 method only accounts for updrafts, an approach later modified to include downdrafts in the Conditional Eddy Accumulation method (TH08b; Zahn et al., 2024). Another expansion of TH08 was introduced when Zahn et al. (2022) created the Conditional Eddy Covariance method (ZN22) by stating that conditions within O1 were not equal to soil evaporation but were instead proportional. They then define a second octant (O2) for when w' and q' are greater than 0 and c' is less than 0 to represent transpiration conditions. Then conditional covariances can be computed for E and T:

$$f_E = \frac{1}{N} \Sigma I_E w' q' , \tag{13}$$

$$f_T = \frac{1}{N} \Sigma I_T w' q' , \tag{14}$$

Where I_E and I_T are indicator functions equal to either 1 or 0 depending on if the data falls within O1 or O2. Because of the assumption that f_E and f_T are representative of the stomatal and non-stomatal fluxes, the ratio of f_E to f_T is then equal to the ratio of E to T. This approach was later modified to include WUE, if known, to help further constrain the carbon flux (ZN22b; Zahn et al., 2024). However, due to the need for high frequency datasets and the high computational time both TH08 and ZN22 require, they can be difficult to apply to flux sites and thus have been infrequently chosen as the preferred ET partitioning method. Another limitation of all high frequency-based methods (SK10, TH08, and ZN22) is that because they distinguish stomatal and non-stomatal sources of water vapor based on the q-c correlation, interception evaporation from the canopy surface can be incorrectly represented in the transpiration estimates and therefore these methods should not be applied in ecosystems with consistent or frequent rainfall (Ranjbar et al., 2026; Shih et al., 2025; Zahn et al., 2022).

However, Ranjbar et al. (2026) introduced a machine learning method (RB26) that uses high frequency data to partition ET not just into T and E but also partitions E into direct evaporation and interception evaporation. This knowledge-guided neural network trains against T estimates from TH08b and utilizes activation functions to constrain the estimates to realistic values. Uniquely, interception evaporation is only allowed to be estimated by the model within 24 hours of rainfall or when dew has recently formed and the model forces mass and energy conservation laws to be met in the estimates. In testing, it has been able to keep interception evaporation out of the transpiration estimates unlike the other high frequency methods, however it has been largely validated against other high frequency-based methods and showed high agreement with estimates from TH08b which would be expected as the model is trained on prior TH08b estimates.

3.1.5 Linear regression

The method introduced by Scott & Biederman (2017) (SB17) uses linear regression on multiyear datasets to derive a direct relationship between measured annual ET and gross ecosystem photosynthesis (GEP where GEP = −GPP) where the x-intercept represents an average E estimate when GEP = 0. Then by inverting the regression whereby GEP serves as a predictor of ET, they define the slope of the regression as the marginal ecosystem WUE (WUE_{mar}), which is then used to calculate T by:

$$T = mxGEP, \tag{15}$$

Where m is the inverse of WUE_{mar} (WUE_{mar}^{-1} = ΔET/ΔGEP) and x is the ratio between the inverse of transpirational WUE (T/GEP) and WUE_{mar}^{-1}. Because the regression is defined from periods without transpiration, interception evaporation is accounted for in E estimates. There is also no need for the assumption T/ET approaches 1 in SB17, unlike with the uWUE methods, because potential WUE, or WUE_{mar}, is calculated on an average monthly basis by comparing multiple years of data. This makes SB17 more applicable to water-limited sites, however, the site must display consistent ecological response progressions between years in order for the monthly estimate of WUE_{mar} to accurately represent the ecosystem (Eichelmann et al., 2022; Hu and Lei, 2021; Reich et al., 2024; Scott and Biederman, 2017).

While this method is more accessible as it does not require high frequency data or a priori plant WUE information, it does require a minimum of 3 years of data, with ideal data sets of at least 5-7 years in length in order to produce reliable results

(Eichelmann et al., 2022; Li et al., 2019; Scott and Biederman, 2017). This method also relies on the assumption of a strong relationship between yearly ET and GEP, which is not valid in ecosystems with high water availability (Hu and Lei, 2021; Scott and Biederman, 2017).

Because of the aggregation of data over years, SB17 inherently suppresses the influence of rainy periods, making it unsuitable for dryland ecosystems where an influx of precipitation causes substantial changes in ecosystem processes (Reich et al., 2024). A variation of SB17 was introduced by Reich et al. (2024) who created a semi-mechanistic model in a Bayesian framework called the Dynamic Evapotranspiration Partitioning Approach for Rapid Timescales (SB17b). SB17b operates similarly to SB17 but at a finer temporal scale and estimates weekly WUE by constraining abiotic evaporation and calculating ET and T on daily timescales:

$$ET_{daily} = m_{w(d)} GPP_d + E'_d \, , \tag{16}$$

$$T_{daily} = m_{w(d)} GPP_d \, , \tag{17}$$

Where E'_d is the intercept of the regression (i.e. value of ET when GPP = 0), $m_{w(d)}$ is the inverse of weekly WUE, and GPP_d is daily GPP. While SB17 assumed that E is invariant across years of data for an individual month, SB17b allows E to vary on daily timescales, introducing the influence of rainy periods on T, E, and WUE, and like SB17, interception evaporation is included in E estimates. However, the model uses process-based equations to parameterize abiotic evaporation where the equations do not account for vegetation cover and therefore are unable to represent the full heterogeneity of a tower's footprint (Reich et al., 2024).

3.2 Geographic and climatic distribution of studies applying reviewed ET partitioning methods

Tables summarizing published studies (site location, biome, T/ET results, and comparisons to other methods) using six of the most widely applied EC-based partitioning methods (ZH16, LI19, PP18, TEA18, SK10, SB17) are shown in the appendix (Tables A1-A6), including a table for methods with limited application ($N_S \leq 5$) (Table A7). If a study used more than one partitioning method, it was repeated in each applicable table with a note as to how the results compared between the methods. In instances where studies applied a partitioning method but did not give results including T/ET, T, E, and/or ET quantities, a qualitative summary of important findings was included as well. As there were limited studies presenting paired results from two or more partitioning methods on the same dataset, the following comparison refers to average ecosystem type results and is not representative of how method estimates compare directly unless otherwise stated.

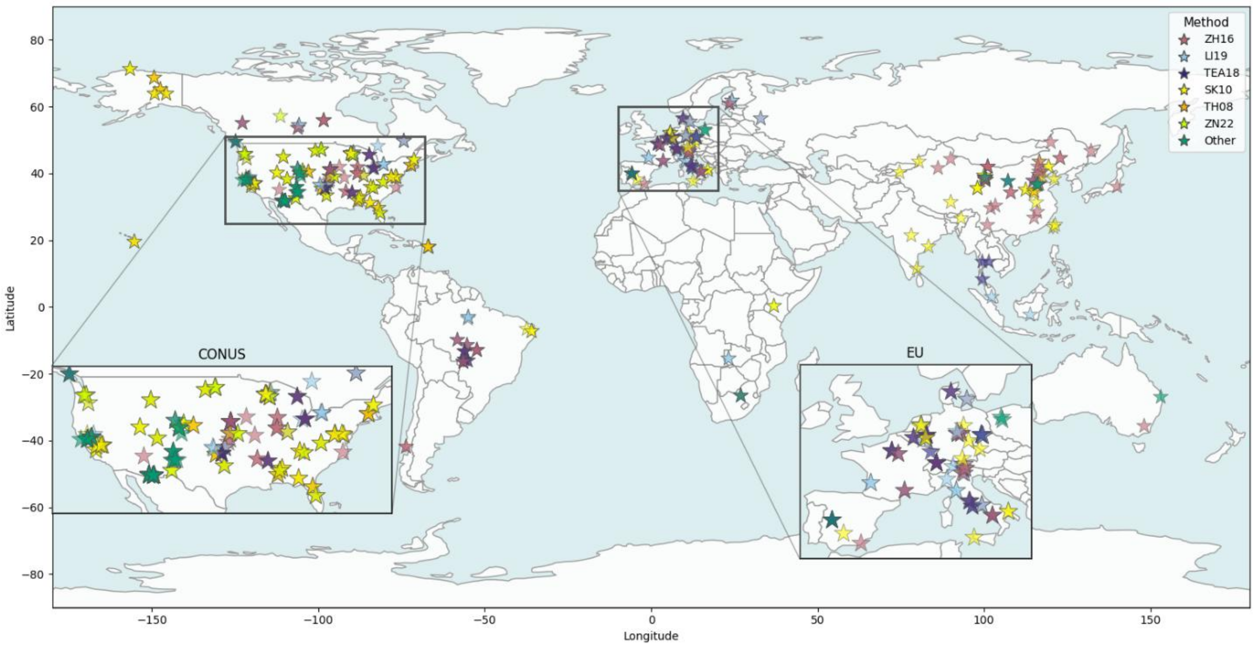

Figure 2: Geographical locations of data records found in literature search. Stars are opaquer in cases where multiple studies have been carried out on the same site while a site with a single study would have a slightly transparent star. Method types: underlying water use efficiency: ZH16, stomatal conductance: LI19, machine learning: TEA18, high frequency: SK10, TH08, ZN22. “Other” comprised the following method types: underlying water use efficiency: BH16, stomatal conductance: PP18, machine learning: EE22, linear regression: SB17 and SB17b. Global studies featuring more than 50 sites across 4 continents are not featured on the map. CONUS: continental United States, EU: Europe, ZH16: Zhou et al. (2016), LI19: Li et al. (2019), PP18: Perez-Preigo et al. (2018), TEA18: Nelson et al. (2018), SK10: Scanlon & Kustas (2010), SB17: Scott & Biederman (2017), BH16: Berkelhammer et al. (2016), EE22: Eichelmann et al. (2022), TH08: Thomas et al. (2008), ZN22: Zahn et al. (2022), SB17b: Reich et al. (2024).

Table 2: Mean and standard deviation of transpiration to evapotranspiration ratios (T/ET) calculated in published studies using EC-based ET partitioning methods (only methods with total $N_R>5$ are shown). Quantitative results of annual and growing season means reported in Tables A1-A6 were used for calculating the average (Avg) and standard deviation (STD). For croplands (CRO), if two or more crops were reported on in the same study, they were each represented as an individual record. Studies reporting on several biomes without distinction were represented in Misc. Global studies featuring more than 50 sites across 4 continents were not included in the calculations as individual T/ET estimates were not reported for each N_R. The plant functional types (PFT) of the ecosystems were identified with GRA: grassland, DBF: deciduous broadleaf forest, ENF: evergreen needleleaf forest, EBF: evergreen broadleaf forest, MF: mixed forest, SAV: savanna, WSA: woody savanna, OSH: shrubland, BSV: bare sparse vegetation, WET: wetland. N_R: number of records identified, uWUE: underlying

water use efficiency. Method abbreviations: ZH16: Zhou et al. (2016), LI19: Li et al. (2019), PP18: Perez-Preigo et al. (2018), TEA18: Nelson et al. (2018), SK10: Scanlon & Kustas (2010), SB17: Scott & Biederman (2017).

Method type	**Method**	**T/ET**	GRA	EBF	CRO	ENF	MF	WET	DBF	SAV	OSH	WSA	BSV	Misc.
uWUE	ZH16	N_R	16	1	28	8	3	1	8	2	4	2	1	4
		Avg. (STD)	0.52 (0.12)	0.52	0.51 (0.11)	0.48 (0.05)	0.49 (0.10)	0.49	0.49 (0.04)	0.48 (0.13)	0.42 (0.16)	0.42 (0.04)	0.37	0.49 (0.08)
Stomatal conductance	LI19	N_R	2	1	3	1	0	1	2	0	0	1	0	2
		Avg. (STD)	0.67 (0.16)	0.54	0.55 (0.10)	0.75	-	0.56	0.58 (0.31)	-	-	0.61	-	0.70 (0.05)
	PP18	N_R	0	0	2	1	0	2	0	0	0	1	0	1
		Avg. (STD)	-	-	0.66 (0.28)	0.55	-	0.29 (0.08)	-	-	-	0.60	-	0.45
Machine learning	TEA18	N_R	4	1	11	3	1	0	6	3	2	2	0	3
		Avg. (STD)	0.64 (0.12)	0.78	0.70 (0.14)	0.68 (0.60)	0.51	-	0.71 (0.06)	0.69 (0.08)	0.47 (0.18)	0.69 (0.03)	-	0.67 (0.09)
High frequency	SK10	N_R	3	0	18	1	0	1	3	0	0	0	0	1
		Avg. (STD)	0.56 (0.20)	-	0.67 (0.09)	0.53	-	0.46	0.73 (0.17)	-	-	-	-	0.52
Linear regression	SB17	N_R	2	0	2	0	0	0	1	2	2	0	0	0
		Avg. (STD)	0.59 (0.11)	-	0.67 (0.04)	-	-	-	0.40	0.68 (0.09)	0.47 (0.04)	-	-	-

ZH16 has been studied in all major biome types across all continents (excluding Antarctica) across 58 studies (Tables 2, A1; Fig. 2). The majority of reported results (N_R) were in croplands (32) representing a variety of annual and perennial crops (e.g. soybeans, rice, cotton, wheat, maize, etc.). Grasslands (24) and forests (34 across all forest types) were also frequently reported on. ZH16 was applied the most in Asian (34) and North American (18) sites (Fig. 2) and was included in four global studies (Cao et al., 2022; Chang et al., 2025; Nelson et al., 2020; Xue et al., 2023). SK10 usage was reported in 40 studies, mostly in croplands (29) with an emphasis in wheat (8), maize (6), and various orchards (6). SK10 was also heavily applied across different forest types (11) and in North America (20) however several continents and biomes have not yet been included (Tables 2, A5; Fig. 2). TEA18 was the next most frequently applied method, appearing in 22 studies, including 3 global studies (Table A4) (Chang et al., 2025; Nelson et al., 2020; Xue et al., 2023). Like SK10 and ZH16, TEA18 was applied the most in forests (16) and croplands (12) and across Asia (8) and North America (7; Fig 2).

The remaining methods had a considerable drop in number of studies where PP18 and LI19 were used in 6 and 8 studies, respectively, however both methods were included in global studies (Tables A2, A3) (Chang et al., 2025; Maes et al., 2020; Nelson et al., 2020). The next highest applied method being SB17 featured in 7 papers where 6 were in North America (Table A6; Fig. 2). The BH16 method was used in 5 studies, predominately in North America (3; Table A7, Fig. 2), 3 of which were in evergreen forests (mean = 0.66). The high frequency methods from ZN22 and TH08 were used in 5 and 3 identified studies, respectively (Table A7) and while they often agreed with each other, both tended to be higher than SK10 estimates. EE22 has been applied in 3 studies, 2 in North America and once in Asia (Table A7, Fig. 2). SB17b and RB26 were both only applied in one North American study, and a combined method of ZH16 and SB17 was used once in a GRA / WSA ecosystem in North America (Table A7; Yuan et al., 2021).

3.3 Comparison of ET partitioning method results from identified studies

ZH16 and PP18 consistently produced the lowest T/ET values when compared to other EC-based partitioning methods (Figs. 3, 4; Tables 2, A1, A3). While ZH16 was applied in significantly more studies, both were compared on a global scale (Nelson et al., 2020) so low estimates can be concluded to be produced on a systemic basis from both methods. In regionalized studies, ZH16 predicted lower estimates across croplands, evergreen needleleaf forests, and woody savannas than PP18 although this comparison is pulled from several studies across several sites as opposed to direct comparisons of methods on the same dataset (Fig. 3).

On the other hand, TEA18 estimates consistently had either the highest or comparable T/ET value estimates when directly compared to other EC-based methods in 18 of 18 studies (Table A4, Figs. 3, 4). Within this pool of studies were three global analyses where TEA18 was applied to EC sites across diverse ecosystems and produced higher T/ET estimates than ZH16, PP18, and LI19 in every biome with reported values across all studies (Chang et al., 2025; Nelson et al., 2020: Xue et al., 2023). These high estimates agreed well with many non-EC based partitioning methods (i.e., sap flow, two-stage theory of bare soil evaporation, TSEB-SM, and LSMs). High frequency methods estimated high T/ET values as well, although still lower than TEA18, with common summer trends showing ZN22 > TH08 > SK10 (Fig. 3; Table A5, A7). Linear regression-based methods (SB17 and SB17b) had limited testing, which is in part due to the hefty requirement of ideal datasets have 5-7 years of data. However, from the 7 studies they have been applied collectively, SB17 produced mid-range and SB17b produced high T/ET estimates when compared to other method types (Tables A6, A7). LI19, a stomatal conductance method, also produced mid-range T/ET values compared to other methods (Table A2) while BH16, the other uWUE-based method, had no discernible trends regarding magnitudes of estimates across 5 studies.

When focusing on global T/ET estimates, five studies presented a mean annual T/ET estimate across at least four biomes using at least 50 sites. ZH16 presented an average global annual T/ET of 0.50 ± 0.06 (N_S=4; Cao et al., 2022; Chang et al., 2025; Nelson et al., 2020; Xue et al., 2023), TEA18 with 0.67 ± 0.07 (N_S=3; Chang et al., 2025; Nelson et al., 2020; Xue et al., 2023), PP18 with 0.45 (N_S=1; Nelson et al., 2020), and LI19 with 0.64 ± 0.03 (N_S=2; Chang et al., 2025; Maes et al., 2020). These global estimates agreed with the trends of magnitudes produced from each method in regional studies with low estimates from ZH16 and PP18, moderate estimates from LI19, and the highest T/ET estimates from TEA18. The global, annual mean of T/ET across the 4 methods in 5 studies was 0.573 ± 0.10 (Fig. 3). This is comparable to the average T/ET value (0.581 ± 0.14) found from all records regardless of partitioning method or ecosystem (Fig. 3).

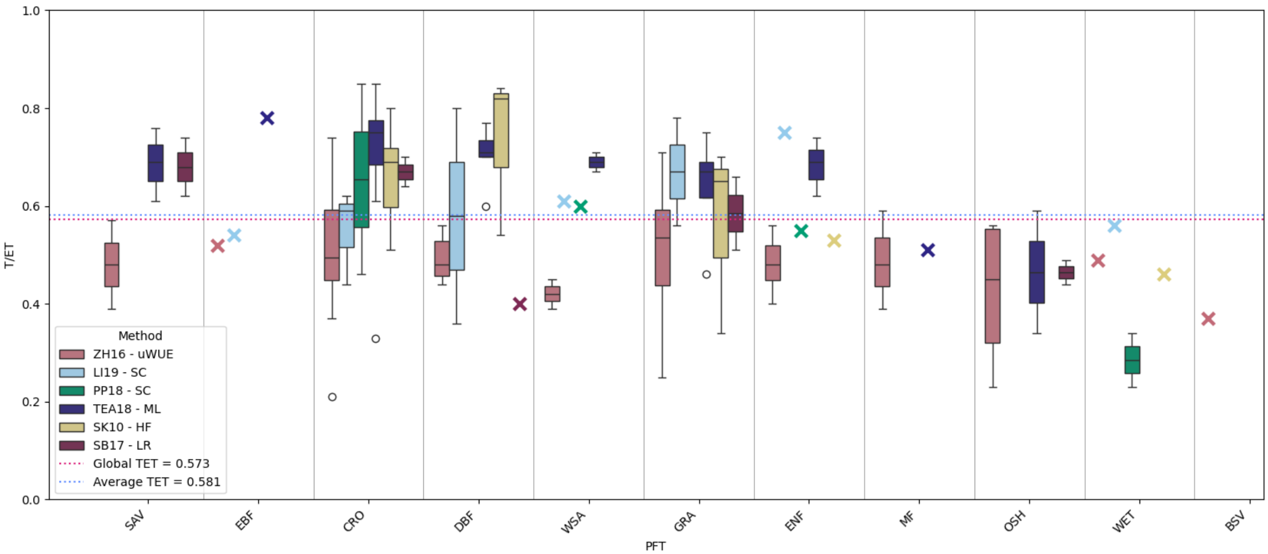

Figure 3: Box and whisker plots of ET partitioning methods estimates across plant functional types (PFT) from all quantitative data extracted from the literature search. Method and PFT combinations with only 1 record are shown as an X. Only methods with more than 5 records are included. PFTs are ordered by decreasing average T/ET estimates across records. The red dotted line is the global T/ET value estimated from studies that included multiple ecosystem types across more than 50 sites. The average T/ET value represents all records from all studies and is shown in the blue dotted line. Methods: ZH16: Zhou et al. (2016), LI19: Li et al. (2019), PP18: Perez-Preigo et al. (2018), TEA18: Nelson et al. (2018), SK10: Scanlon & Kustas (2010), SB17: Scott & Biederman (2017). Method types: uWUE: underlying water use efficiency, SC: stomatal conductance, ML: machine learning, HF: high frequency, LR: linear regression. SAV: savanna, EBF: evergreen broadleaf forest, WSA: woody savanna, CRO: cropland, DBF: deciduous broadleaf forest, ENF: evergreen needleleaf forest, GRA: grassland, MF: mixed forest, OSH: open shrubland, WET: wetland, BSV: bare sparse vegetation.

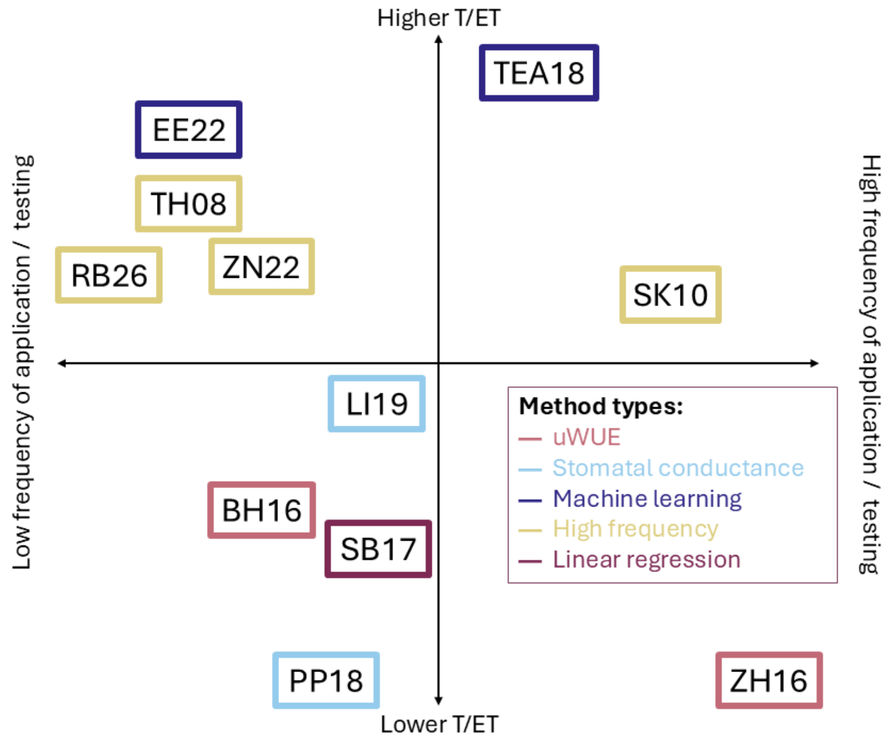

Figure 4: Summarized results of relative T/ET output from the 11 independent methods identified in this review and the frequency of their application and testing against non-EC-based estimates. Methods were placed on the x-axis according to number of studies with methods left of the origin appearing in less than 10 studies and compared to independent measurements in 3 or less instances. Y-axis placement was determined by relative T/ET estimates compared across all studies featuring two or more identified methods. Methods: ZH16: Zhou et al. (2016), BH16: Berkelhammer et al. (2016), LI19: Li et al. (2019), PP18: Perez-Preigo et al. (2018), TEA18: Nelson et al. (2018), EE22: Eichelmann et al. (2022), SK10: Scanlon & Kustas (2010), TH08: Thomas et al. (2008), ZN22: Zahn et al. (2022), RB26: Ranjbar et al. (2026); SB17: Scott & Biederman (2017). uWUE: underlying water use efficiency.

3.3.1 Spatial and temporal drivers of T/ET

LAI and similar vegetation indices were found to be the most common identified driver of T/ET in the studies included in this review (Li et al., 2024d; Lowry et al., 2021; Restrepo-Coupe et al., 2023; Sun et al., 2020; Wagle et al., 2020; Wang et al., 2016a; Zahn et al., 2022; Zhou et al., 2016). While LAI influenced the temporal variability of T/ET within a site/ecosystem, the spatial variability of T/ET presented that a higher LAI did not always indicate higher transpiration rates across sites/ecosystems, as the highest T values were found in SAV ecosystems and relatively low T was estimated for MF (Fig. S1). SWC, especially during dry conditions, was also found to be one of the most important temporal drivers of T/ET in several studies across global biomes (da Rocha et al., 2022; Liu et al., 2022b; Nie et al., 2021). A tall grass prairie study found that

T/ET was strongly positively correlated with sub surface SWC, as roots were able to access underground water sources, and slightly negatively correlated with upper layer SWC as surface water tended to be dedicated to soil evaporation, agreeing with results from GRA and DBF studies (da Rocha et al., 2022; Deb Burman et al., 2022; Scott et al., 2021; Xu et al., 2021). Air temperature and VPD were also found to have significant impacts on the temporal variability of T/ET values and trends across studies (da Rocha et al., 2022; Eichelmann et al., 2022; Nie et al., 2021; Sun et al., 2020; Xu et al., 2021). Across biomes, transpiration ratios were found to be the highest in savannas and evergreen broadleaf forests while the lowest ratios occurred in wetlands and deserts (Fig. S1).

4 Discussion

4.1 Identified partitioning methods and common uncertainties

Our systematic literature review identified 11 independent ET partitioning methods applied across 129 studies spanning 11 plant functional types. Despite their diversity, these methods converge on a small set of core mechanistic principles. The most prevalent approach leverages optimality theory and WUE assumptions to estimate T/ET. Several methods employ WUE-based frameworks: the uWUE methods (ZH16 and BH16) apply optimality assumptions directly, while PP18 (a stomatal conductance approach) embeds optimality into the broader model structure. Linear regression-based methods (SB17 and SB17b) and TEA18 also capitalize on the established ecosystem-scale relationship between GPP and ET to derive T estimates. As such, these approaches (ZH16, BH16, SB17, SB17b, TEA18) all isolate periods when GPP:ET relationships approximate GPP:T relationships (reflecting ecosystem WUE) by filtering data with percentile thresholds. SK10 and ZN22b also incorporate WUE, though high frequency data allows them to derive leaf-level WUE directly from CO_2 and H_2O mixing ratios as opposed to ecosystem WUE like the half-hourly methods. These ties of functionality between different method types draw attention to the prevalence of using known characteristics of stomatal function when considering ecosystem T dynamics. Moreover, the methods' common shared reliance on percentile filtering and straightforward statistical relationships demonstrate efficient strategies for processing large, multi-site, multi-year datasets.

The two methods based on the concept of uWUE predicted low estimates of T/ET across all ecosystems while machine learning methods (both TEA18 and EE22) consistently estimated higher values when compared to other methods (Figs. 3, 4). The magnitude discrepancy between EC-based methods, particularly between ZH16 and TEA18, may be due to the assumption that WUE is optimized at the leaf-level, however, this assumption has a weak theoretical basis (Nelson et al., 2020). ZH16 estimated WUE using a 95th percentile threshold on the relationship between GPP x VPD$^{0.5}$ and ET while TEA18 used the 75th percentile. The upper values in the 95th percentile may have led to an overestimation of WUE and subsequent underestimation of T. One study tested ZH16 using an 80th percentile alongside the more common 95th percentile, and while T/ET estimates were higher with the 80th (0.65 vs 0.47 in a grassland), both regressions still produced estimates lower than SB17 (Ma et al., 2020). While the uWUE methods predicted the lowest T/ET estimates among EC-based methods, when compared to independent methods, values were similar to many modelled values from LSMs, mechanistic, and hydrological models (Bai et al., 2019; Bu et al., 2024; Cao et al., 2022; Jin et al., 2022; MacBean et al., 2020; Song et al., 2021; Wu and Wang, 2025; Xu et al., 2024; Yu et al., 2022). Regardless of their general agreement with models built on similar underlying assumptions, predicted values from ZH16 were underestimated when compared to remote sensing-based products as well as when validated against the isotope method (Bai et al., 2019; Bu et al., 2021; Liu et al., 2022; Song et al., 2022, 2023; Tong et al., 2019; Xue et al., 2023). TEA18 estimates on the other hand agreed well with most ecosystem models, remote sensing-based models, and sap flow measurements though had higher values than an isotope study and an LAI-based model (Bastos Campos et al., 2025; Hu and Lei, 2021; Liu et al., 2022, 2025; Nelson et al., 2018; Xue et al., 2023; Yang et al., 2025). This variety of agreement against non-EC-based methods underscores the importance of comparing several partitioning methods on a dataset as well as collecting more robust ground truth validation to resolve T/ET and determine which ET partitioning methods, both EC-based and otherwise, are producing reliable T estimates.

Comparing the limitations of the partitioning methods, perhaps the most prevalent is the use of GPP in T estimates. GPP is itself a modelled value as EC cannot directly measure GPP just as it cannot directly measure T. So, NEE partitioning methods are used to estimate GPP (Lasslop et al., 2010; Reichstein et al., 2005). However, this means that any uncertainties and biases in the modelled GPP are inherently linked to the subsequent modelled T. The methods that use binned GPP or GPP percentiles (i.e., ZH16, TEA18, LI19, and BH16) will be greatly affected by short-term errors of GPP if they introduce enough outliers to skew the regression. However, they will not be impacted by consistent, systematic GPP alterations as shown by the fact that T estimates were not affected when the nighttime and daytime NEE partitioning methods were tested (Nelson et al., 2020). PP18 on the other hand uses GPP to directly calculate ecosystem stomatal conductance which is then used to estimate T and therefore will be sensitive to both short-term and systematic GPP biases and errors. Additionally, the lack of agreement between GPP-based methods may indicate that the assumed optimal relationship between stomatal carbon gain and water loss is not maintained across diverse ecosystems and in fact, that the relationship varies by plant type and is changing with the warming climate (Hatfield and Dold, 2019; Medlyn et al., 2017; Nelson et al., 2020).

Many of the methods are not suited for heterogenous ecosystems. Any method that assumes an optimal relationship between carbon gain and water loss at the leaf level (ZH16, BH16, PP18) oversimplifies the dynamicity of WUE with seasonal variations in CO_2, a property most apparent among varying vegetation types (Zhou et al., 2016). The high frequency methods assume all transpiration is coming exclusively from plant leaves, another assumption with the potential to be violated in heterogenous ecosystems (Reich et al., 2024; Scanlon and Kustas, 2010). In ecosystems with sparse vegetation, methods that assume ET approaches T (ZH16, BH16, TEA18) should only be applied after careful consideration as soil evaporation can generally not be ignored in ecosystems with low leaf area (Nelson et al., 2018; Zhou et al., 2016). Another source of large uncertainties is the handling of interception evaporation between the methods. The stomatal conductance-based methods ignore this process completely even with studies reporting that 8.5-10% of annual rainfall is intercepted by plant surfaces globally with some regional estimates reaching up to 50% depending on ecosystem type (Fischer et al., 2026; Lian et al., 2022; Zhong et al., 2022). EE22 does not remove wet periods from the training data like TEA18, however it still neglects to account for daytime interception rates that differ from their nocturnal counterparts (Czikowsky and Fitzjarrald, 2009). In high frequency methods, the inattention to rainfall often results in interception evaporation being incorrectly partitioned into T which may be in part responsible for this method type's high T/ET estimates (Fig. 4). The methods which do appropriately attribute interception to E, whether directly or by means of using GPP to estimate T, still face uncertainties as EC systems often underestimate the water flux of an ecosystem during precipitation (Van Dijk et al., 2015; Fischer et al., 2026). ET measurements from EC during rain are inherently biased adding additional uncertainties to ET partitioning estimates and correcting ET measurements to account for this leads to contradicting changes in T/ET depending on which method was applied (Zhang et al., 2023). This again emphasizes the importance of applying multiple partitioning methods for comparisons in studies to see where T/ET estimates are most uncertain.

Even so, these method assumptions and limitations still lend themselves to more reliable applications in some ecosystems over others, even without rounds of robust ground truth validations. Many method types (uWUE, stomatal conductance, high frequency, and linear regression) favor homogenous ecosystems, making TEA18 a better option when partitioning in forest ecosystems. EE22, the other machine learning-based method, may also be able to partition ET in forest ecosystems, but only at sites that can verify negligible nocturnal transpiration. EE22 is, however, the best suited for wetland ecosystems as it estimates T independently of ecosystem carbon dynamics and WUE. The linear regression-based methods, SB17 and SB17b, have assumptions well suited to dryland ecosystems, but should not be used in rotational croplands where annual trends of GEP and ET vary by year and by crop type. The high frequency methods have, however, been applied heavily in croplands as they assume all T comes from plant leaves and function well in homogenous environments. If a researcher does not have access to high frequency data or lacks the computational resources to complete the partitioning, TEA18, the stomatal conductance methods (LI19 and PP18), and the uWUE methods (ZH16 and BH16) can all be applied and compared in croplands as well. Grasslands also lend themselves to the assumptions of the uWUE and stomatal conductance methods although neither group of method types can handle ecosystems with sparse vegetation or extensive heterogenous ecosystems like drylands or forests. However, to confidently determine which methods should be used in which biomes, more studies that test 2 or more partitioning methods on the same dataset, especially studies that can compare those results to ground truth data, are necessary.

4.2 Global application of ET partitioning methods

ZH16, SK10, and TEA18 have been utilized to partition ET in many studies (N_S = 58, 40, and 22, respectively) across even more datasets. However, while 15 LI19 T/ET estimates have been reported across 8 studies, every other method has reported less than 10 studies. Even though LI19 and PP18 were applied in global studies and therefore have been utilized in diverse biomes, this limited range of experiments, especially rare instances where several methods have been applied to the same data record for comparison or validated against independent observations, emphasizes the need for further testing of all methods across all PFTs in order to pair T/ET estimates, fully evaluate the performance of each method, and reliably track global T trends (Fig. S2).

However, while direct comparisons of method estimations at specific EC sites are limited, there were still 5 identified studies that presented global T/ET values (Cao et al., 2022; Chang et al., 2025; Maes et al., 2020; Nelson et al., 2020; Xue et al., 2023). From these 5 studies presenting 10 estimates, an average annual T/ET value of 0.573 ± 0.10 was determined (Fig. 3). This value was comparable to the average T/ET value calculated from every identified record in the literature search (T/ET = 0.581 ± 0.14; Fig. 3). While these averages were calculated independently, their correlation suggests an even representation of PFTs in accordance with their abundance were identified in the search.

The global values found in this study as well as the average T/ET value are consistent with a study using remote sensing data paired with an LSM and LAI measurements (0.57 ± 0.07; Wei et al., 2017), a satellite SIF based method (0.57 ± 0.14; Liu et al., 2022c), a hydrological LSM (0.59; Wang-Erlandsson et al., 2014), and similar to a lateral flow based model (0.62 ± 0.12; Maxwell & Condon, 2016), the CMIP5 model (0.62 ± 0.06; Lian et al., 2018), and a previous synthesis study combining EC, sap-flow and isotopic partitioning methods (0.61 ± 0.15; Schlesinger & Jasechko, 2014). This study also falls within the bounds of an isotopic synthesis study (0.35-0.80; Coenders-Gerritis et al., 2014) which adjusted previous uncertainty assumptions regarding isotopes where they reported a global T/ET range of 0.80-0.90 (Jasechko et al., 2013), and another synthesis using T, E, ET, with LAI data (0.38-0.77; Wang et al., 2014). A mechanistic ecohydrological model, the remote sensing GLEAM model, the TSEB-SM, and satellite water vapor isotope measurements all found slightly higher global terrestrial T/ET values at 0.70 ± 0.09, 0.80, 0.73, and 0.64 ± 0.13, respectively (Fatichi and Pappas, 2017; Miralles et al., 2011; Paschalis et al., 2018; Xue et al., 2023).

4.3 Transpiration trends and drivers

The dynamics of T/ET differed on diurnal, seasonal, and interannual timescales due to varying leaf area index (LAI), plant cover, and environmental conditions (Scott & Biederman, 2017). In regard to evolving global T trends, Xue et al. (2020) used ZH16 and found 12 of 67 flux sites had significant changes in T/ET over the past two decades seeing 5 sites with decreased T/ET and 7 sites with increased T/ET. They also found no consistent trends across biomes concerning LAI's influence on T/ET dynamics regardless of SWC. This contradicted many regionalized studies that repeatedly found LAI to be one of the most important drivers for ecosystem T (Li et al., 2024d; Lowry et al., 2021; Restrepo-Coupe et al., 2023; Sun et al., 2020; Wagle et al., 2020; Wang et al., 2016a; Zahn et al., 2022; Zhou et al., 2016). The reliance on LAI is not only present in EC-based partitioning studies but also when using remote sensing based machine learning models, ecosystem resistance models, a method based on EC measurements with LSM data, and isotopic methods (Chen et al., 2024; Fatichi and Pappas, 2017; Gnanamoorthy et al., 2024; Good et al., 2014; Hu et al., 2026; Lu et al., 2023; Schlesinger and Jasechko, 2014; Wang et al., 2014). In fact, LAI and other similar vegetation indices can explain around 40% of annual variability in global T/ET (Wang et al., 2014; Wei et al., 2015). Significant impacts were seen on seasonal timescales as well where increased plant cover led to increased T/ET (Li et al., 2019; Scott and Biederman, 2017; Wang et al., 2010; Wei et al., 2015).

Another study found that the presence of drought increased global T/ET due to decreased soil evaporation from limited water availability (Yang et al., 2025b) which is supported by findings of the influence of SWC on T in regional studies (da

Rocha et al., 2022; Liu et al., 2022b; Nie et al., 2021; Wang et al., 2024a). Solar-induced chlorophyll fluorescence (SIF), VPD, and soil water content (SWC) have also been found to correlate with annual and seasonal T/ET dynamics on a global scale in various ecosystem models informed from remote sensing, sap flow, or LAI data (Li et al., 2024a; Pagán et al., 2019; Song et al., 2023a; Wei et al., 2017). However, even with known T/ET drivers, global estimates of T/ET still suffer from large uncertainties varying anywhere from 24-90% depending on the partitioning method used (Wei et al., 2017). More studies directly comparing several partitioning approaches on the same datasets are required to fully compare the methods so that a systematic framework for selecting an appropriate partitioning method can be established for future studies.

5 Conclusions and Recommended Future Directions

By conducting a comprehensive literature search for eddy covariance-based evapotranspiration partitioning methods, 11 independent methods were found to be applied across 129 studies. Two methods partition ET by assuming there is an optimal, linear relationship between ET and GPP x $VPD^{0.5}$. Methods built from ecosystem conductance models also use the relationship between ET, GPP, and VPD, but there are no linear assumptions allowing the relationship to vary with vegetation type. For other methods using half-hourly EC data, two use machine learning to make T estimates from flux and meteorological data while one assumes a linear relationship between ET and gross ecosystem production. There were also 4 methods requiring high frequency EC data that assumed similar transport of non-stomatal and stomatal turbulent fluxes. All of the assumptions on which the various methods are based are ecosystem-dependent and no single method seems to be able to produce reliable T/ET estimates across all biomes. As such, method selection still must be guided by a priori site knowledge of vegetation characteristics, environmental conditions, and data availability.

Leaf area index was the most consistent driver of T/ET values and trends across studies with soil water content, VPD, and air temperature also playing significant roles depending on ecosystem type. From the identified studies, a global mean T/ET of 0.58 was calculated. This value is comparable to previous global studies using land surface models, remote sensing data, and isotopic partitioning approaches. This agreement lends confidence to the ability of eddy covariance-based methods to capture ecosystem-scale ET partitioning even with common disadvantages among the methods such as the reliance on GPP estimates and the neglect of interception evaporation. However, while global studies, both eddy covariance-based and other, are converging on an annual T/ET estimate from terrestrial ecosystems, most T/ET estimates, regardless of their method of origin, remain largely unvalidated against ground truth measurements.

Currently, only 3 methods have been included in more than 10 studies and while North America, Europe, and Asia are well represented in the datasets, Africa and Oceania have been included in very few partitioning studies. Evergreen broadleaf forests and mixed forests also have limited testing; however, croplands and grasslands are well represented. To improve our understanding of ecosystem T dynamics and clearly define when and where each method should be applied, researchers would benefit from more publicly available validation datasets. Whether from lysimeters, sap flow measurements, or other ground truth data sources of E and/or T, all will help to constrain the magnitudes of T/ET estimates across methods and increase confidence in ET partitioning. Additionally, more studies focused on the relationship between water loss and carbon uptake from the stomatal-to leaf-to ecosystem level are needed to verify or adapt our current understanding of when and where the optimal WUE assumption holds. More accessible, high frequency data and more open-source code will allow for easier applications of methods and more studies comparing several partitioning methods against the same datasets will also help to better define a protocol for choosing a method for future partitioning studies. Further testing of all methods, especially newly established methods and additional studies in underrepresented regions and ecosystem types will give improved insights into how assumptions for each method hold in various ecosystems and provide information into changes of T and E under a warming climate.

6 Appendix A

6.1 ZH16

Table A1: Studies that have used the underlying water use efficiency partitioning method by Zhou et al. (2016) to calculate the transpiration to evapotranspiration ratio (T/ET). The timescales used in the T/ET calculations are listed as well as any comparisons to other ET partitioning methods. Locations are listed by FLUXNET site IDs when applicable, for any non-FLUXNET sites, the location is listed in accordance to how it was reported in the methods of each study. The plant functional types (PFT) of the ecosystems are identified with CRO: cropland, GRA: grassland, DBF: deciduous broadleaf forest, ENF: evergreen needleleaf forest, EBF: evergreen broadleaf forest, MF: mixed forest, SAV: savanna, WSA: woody savanna, OSH: shrubland, BSV: bare sparse vegetation, WET: wetland. GS: growing season, LAI: leaf area index, HRB: Heihe River Basin, TSEB: two source energy balance model, TSEB-SM: TSEB aided by soil moisture, LSM: land surface model. Methods: ZH16: Zhou et al. (2016), LI19: Li et al. (2019), PP18: Perez-Preigo et al. (2018), TEA18: Nelson et al. (2018), SK10: Scanlon & Kustas (2010), SB17: Scott & Biederman (2017).

Reference	**PFT**	**Location**	**Calculation**	**T/ET**	**Notes**
(Zhou et al., 2016)	CRO (corn)	US-Bo1, IB1, Ne1, Ne2, Ne3	Annual mean	0.69	
	CRO (soybean)	US-Bo1, IB1, Ne2, Ne3		0.62	
	GRA	US- Arb, Goo, Var, Wir		0.6	
	ENF	CA-NS3, NS5, US-NC2		0.56	
	DBF	US-Ha1, Moz, UMB, WCr		0.52	
(D'Acunha et al., 2024)	CRO (soybean)	Amazon agriculture, Cerrado agriculture Lucas do Rio Verde, Cerrado agriculture Jaciara	From annual T, ET totals	0.43	Lower T/ET estimates than with TEA18 method
	DBF	Amazon forest Tanguro, Amazon forest Sinop, Pantanal forest	Annual mean	0.44	
	GRA			0.44	

	WSA Misc.	Amazon pasture, Pantanal pasture Cerrado Campo sujo All Mato Grosso, Brazil sites (from above)		0.39 0.42	
(Liu et al., 2023)	CRO (rice)	Poyang Lake Basin, Jiangxi Province, China	GS mean	0.47	Lower T/ET estimates with direct seeded early rice vs. transplanted early rice
(Hu et al., 2018)	OSH DBF CRO (cotton) CRO (wheat/maize) GRA	HRB, Sidaoqiao HRB, Xitaizi HRB, Xinier HRB, Daman HRB, Arou	Weekly mean	0.59 0.36 0.63 0.39 ~0.40	
(Nelson et al., 2020)	DBF GRA ENF Misc.	251 FLUXNET sites	Annual mean Peak seasonal	0.45 0.43 0.40 0.52 0.58	Lower T/ET estimates than with TEA18 method, similar estimates to PP18
(Wang et al., 2020)	CRO (maize)	Yangling, Guanzhong Plain, China	GS mean	0.52	
(Peng et al., 2023)	CRO (wheat)	Yangling, Guanzhong Plain, China	GS mean	0.56	
(Hu & Lei, 2021)	CRO (wheat) CRO (maize)	Weishan, North China Plain	GS mean	0.52 0.46	Lower T/ET estimates but similar trends to the two-stage theory of bare soil evaporation, lower estimates than SB17, SK10, and TEA18
(Xu et al., 2021)	GRA ENF CRO (maize) BSV OSH MF	HRB, Arou HRB, Guantan HRB, Daman HRB, Huazhaizi HRB, Sidaoqiao HRB, mixed forest	Annual mean	0.53 0.52 0.59 0.37 0.56 0.59	
(Li et al., 2024d)	ENF	US-GLE	Annual mean	0.45	Decreased T/ET during bark beetle infestation that decreased LAI
(Han et al., 2018)	GRA	CN-NMG	GS mean	0.53	Decreased T/ET during prolonged drought period
(Gan and Liu, 2020)	CRO (maize) ENF GRA CRO (maize/wheat) CRO (orchard)	CN-YK, TYC CN-DYK, QYZ CN-TYG CN-DX CN-MY	Annual mean	0.39 0.46 0.43 0.45 0.44	
(Paul-Limoges et al., 2022)	CRO (wheat) CRO (barley)	CH-Oe2 CH-Oe2	GS mean	0.48 0.37	Decreased diurnal and seasonal T/ET trends than TEA18 method
(Xu et al., 2024)	GRA	HRB, Arou	GS mean	0.54	T/ET values and trends follow SIB2 model (an LSM)
(Chen et al., 2023)	CRO (maize/soybean)	US-Ne1, Ne2, Ne3	GS mean	0.49	T/ET under no-till (0.49) was larger than under plow till management (0.44). Peak T/ET occurred later for soybean vs. maize

(A et al., 2022)	DBF to GRA transition	Hailaer River Basin	Annual mean	0.58	
(da Rocha et al., 2023)	GRA (ungrazed) GRA (grazed)	Rannella Flint Hills Prairie Preserve, Kansas, USA	GS mean	0.71 0.64	
(Liu & Qiao, 2023)	CRO (cotton)	Manas River Basin, Xinjiang, China	Seedling stage Budding stage Blooming and boll stage Boll opening stage Whole stage	0.34 0.61 0.81 0.51 0.61	
(da Rocha et al., 2022)	GRA	US-xKZ	GS mean	0.59	
(Bai et al., 2019)	CRO (maize)	HRB, Daman	GS mean GS peak Irrigation periods	0.74 0.83 0.63	Lower T/ET values than isotope method, similar values to lysimeter method and Shuttleworth-Wallace method
(Chen et al., 2022)	CRO (soybean) CRO (maize) CRO (wheat)	US-Br3, Ne3, Bo1 US-Ne1, CN-Yuc, Daman CN-Yuc, DE-Seh, US-ARM	Annual mean	0.43 0.50 0.38	
(Cao et al., 2022)	Misc.	86 FLUXNET sites	Annual mean	0.59	Similar trends as with Shuttleworth-Wallace and PT-JPL models but with lower inter-site variability
(Reavis et al., 2024)	CRO (rice)	US-HRC, HRA	GS mean	0.47	Lower T/ET with alternate wetting and drying vs. delayed continuous flooding at US-HRC, but the opposite for US-HRA
(Ma et al., 2020)	SAV GRA	US-Ton US-Var	GS mean with regular (95%) regression (with 80% quantile regression)	0.39 (0.61) 0.47 (0.65)	Both regular and 80% quantile regression estimates lower than with the SB17 method. Estimate magnitudes were regular < 80% quantile < SB17
(Raghav et al., 2022)	CRO (wheat)	GRL-FLUXNET sites 1, 2, and 3	GS mean	0.54	Lower T/ET estimates than with SK10 or TEA18 methods
(Scott et al., 2021)	DBF GRA	US-CMW US-Wkg	Annual mean	0.56 0.35	Lowest T/ET estimates in the summer compared to SB17, TEA18, and LI19 methods
(Zhou et al., 2018)	GRA CRO (maize) OSH	HRB, Arou HRB, Daman HRB, Huyanglin	GS mean	0.55 0.63 0.55	
(Jiang et al., 2020)	CRO (wheat) CRO (rice) CRO (soybean)	CH-Oe2, US-ARM, FR-Grl US-Twt, JAN-MSE US-Ne2, Ne3, CRT	Annual mean	0.65 0.57 0.60	

	CRO (maize)	FR-Grl, IT-Bci, US-Ne1		0.67	
(Xue et al., 2023)	CRO EBF ENF DBF GRA MF OSH SAV WSA Misc.	10 sites 6 sites 13 sites 9 sites 11 sites 1 site 2 sites 2 sites 3 sites All (57 sites)	Annual mean	0.21 0.52 0.52 0.55 0.56 0.39 0.23 0.57 0.45 0.44	Across all ecosystems, T/ET from ZH16 and TSEB were lower than estimated from TSEB-SM and TEA18 methods
(Perez-Quezada et al., 2024)	DBF WET	CL-SDF CL-SDP	Annual mean	0.46 0.49	
(Sun et al., 2020)	DBF MF ENF OSH	Mount Gongga, Qinghai-Tibetan Plateau	Annual mean (uWUE estimated with R_{net} in place of VPD)	0.47 0.48 0.50 0.35	
(Wu & Wang, 2025)	GRA	HRB, Arou	GS mean	0.67	Results matched well with the Soil Plant Atmosphere Continuum model
(Zhang et al., 2025a)	CRO (misc.)	US-ARM, CRT, Twt, Tw2, Tw3 IT-BCi, CA2 DE-Seh, RuS, Kli, Geb FR-Gri, FI-Jok, DK-Fou, CH-Oe2, BE-Lon	GS mean	0.48	Lower than TEA18 values (0.66). Both methods estimated the highest values from maize while ZH16 estimated the lowest values from rapeseed and TEA18 from paddy rice
(Chang et al., 2025)	CRO OSH GRA DBF	HRB, Daman HRB-HZZ, HRB-HM HRB-Arou, HRB-DSL HRB-HHL, HRB-SDQ	GS mean	 0.25 0.49	CRO has consistently low values, similar to GRA. OSH values were moderate while the values from the forest were the highest
(Xu et al., 2026)	ENF	Mohe Forest Ecosystem Research Station	GS mean	0.44	
(Wang et al., 2026)	Misc.	368 flux sites	Annual mean	0.45	Lowest global T/ET estimates compared to TEA18 and LI19 but agreed well with sap flow measurements
(Zhang et al., 2025b)	OSH	HRB, Sidaoqiao	GS mean		ZH16 estimates agreed well with sap flow values and the two-source Penman-Monteith model. ZH16 had higher estimates than the two-source Shuttleworth and Wallace (SW) and simplified SW models
(Zheng et al., 2025)	Misc.	72 flux sites	Annual mean		Similar but slightly lower values across ecosystems when compared to SIF-driven semi-mechanistic and hybrid models
(Song et al., 2023b)	CRO	HRB, Daman	GS trend		Estimates from one GS agreed well with the TSEB-SM informed by satellite soil moisture data

(Song et al., 2022)	GRA CRO	HRB, Arou HRB, Daman	GS trend		Estimates from four GS were consistently lower than when compared to the TSEB-SM informed by surface soil moisture data
(Song et al., 2023a)	CRO	HRB, Daman	GS trend		Estimates from two GS were consistently lower than when compared to the TSEB-SIF. Trends followed canopy stomatal conductance
(Song et al., 2021)	GRA CRO	HRB, Arou HRB, Daman	GS trend		Seasonal trends and values of T/ET agreed well with the LSTR model (a RS-based method using land surface temperature reconstruction)
(Liu et al., 2022a)	CRO (maize)	HRB, Daman	GS trend		Similar trends as a remote sensing trapezoid-based estimate informed by LAI and NDVI values. Lower values when compared to isotopes and TEA18
(Bu et al., 2021)	CRO DBF EBF ENF WSA GRA	US-Ne1, Ne2, Ne3, ARM US-Wcr, MMS, DE-Hai AU-Tum CA-Qfo, FI-Hyy US-Wkg US-Var, SRM, AT-Neu, IT-Mbo	Annual trend		Consistently underestimated across CRO, DBF, EBF, ENF, WSA, and GRA sites when compared to TSEB model estimates
(Bu et al., 2024)	GRA SAV	ES-BB, CN-Du2, US-Var, Wkg ES-LM2, US-SRM	Annual trend		Estimates compared well with the CSIF (two-source RS model) when it was modelled with GPP and soil water content data
(Jin et al., 2022)	DBF ENF	DE-Hai, DK-Sor, IT-Col, US-MMS, Wcr CA-Qfo, DE-Tha, IT-Lav, Ren, RU-Fyo, US-GLE, NR1	Annual trend		Similar trends and values when compared to an ecosystem level conductance photosynthesis model using LAI and SWC across all sites
(MacBean et al., 2020)	ENF GRA OSH	US-Fuf, Vcp US-SRM ,SRG, Wkg US-Whs	Annual trend		Similar trends and values for the ENF sites when compared to a soil hydrology-based model. The GRA and OSH sites showed similar trends but lower values compared to SB17 estimates
(Cui et al., 2024)	CRO (kiwi)	Pujiang County, Chengdu Plain, China	Annual trend		Generally lower values than those estimated from an LAI informed conductance model however mid-GS values were similar
(Yu et al., 2022)	CRO DBF EBF ENF GRA	DE-RuS, Seh, US-CRT, Ne1, Ne2, Ne3 CA-Oas, DE-Hai, FR-Fon, US-Ha1, UMB FR-Pue, IT-Cpz CA-NS3, DE-Obe, NL-Loo, US-NR1 DE-Gri, US-Arb, Arc, Goo, SRG	Annual trend		Similar trends when compared to an EC/LSM-based method across global PFTs and TEA18

	WSA	US-SRM, Ton			
(Gnanamoorthy et al., 2024)	EBF	Yunnan Province, China	Annual trend		Similar values and trends to an EC/LSM-based method
(Hao et al., 2024)	ENF	CA-LP1	Annual trend		Lower estimates than from TEA18 but both showed similar trends
(Li et al., 2024e)	ENF	CA-Ca3	Annual trend		Lowest T/ET values when compared to TEA18 and EE22 estimates
(Zheng et al., 2024)	CRO (wheat)	Zhao Xian, Shijiazhuang City, Hebei Province, China	Annual trend		Similar estimates to TEA18
(Räsänen et al., 2022)	SAV	Welgegund, South Africa	Annual trend		Lower values than TEA18, similar values to BH16
(Tong et al., 2019)	CRO (maize)	HRB, Daman	Annual trend		Lower than values from the isotope method
(Li et al., 2024c)	WET	Qixing River National Nature Reserve, Heilongjiang Province, China	Annual trend		E dominated ET, T peaked midday in accordance with GPP
(Guo et al., 2026)	CRO (maize)	Jinzhou Agricultural Ecosystem Field Experiment Site	VPD/SWC trend		T/ET initially decreased then increased with increased SWC. T/ET decreased under high VPD
(Ma et al., 2026)	GRA	26 sites from the China Grassland Transect	VPD trend		T/ET increased as VPD decreased

6.2 LI19

Table A2: Studies that have used the ecosystem conductance partitioning method by Li et al. (2019) to calculate the transpiration to evapotranspiration ratio (T/ET). The timescales used in the T/ET calculations are listed as well as any comparisons to other ET partitioning methods. Locations are listed by FLUXNET site IDs when applicable, for any non-FLUXNET sites, the location is listed in accordance to how it was reported in the methods of each study. The plant functional types (PFT) of the ecosystems are identified with CRO: cropland, GRA: grassland, DBF: deciduous broadleaf forest, ENF: evergreen needleleaf forest, EBF: evergreen broadleaf forest, MF: mixed forest, SAV: savanna, WSA: woody savanna, OSH: shrubland, BSV: bare sparse vegetation, WET: wetland. GS: growing season, LAI: leaf area index. Methods: ZH16: Zhou et al. (2016), LI19: Li et al. (2019), PP18: Perez-Preigo et al. (2018), TEA18: Nelson et al. (2018), SK10: Scanlon & Kustas (2010), SB17: Scott & Biederman (2017).

Reference	**PFT**	**Location**	**Calculation**	**T/ET**	**Notes**
(Li et al., 2019)	ENF	CA-Qfo, SF1, SF2, DE-Obe, FI-Hyy, FR-LBr, IT-Ren, Sro, NL-Loo, US-NR1	Annual mean	0.75	
	CRO	DE-Geb, Kli, FR-Gri, US-ARM, Ne1, Ne2, Ne3		0.62	
	GRA			0.56	

	DBF EBF WSA	AT-Neu, DE-Gri, US-AR1, AR2, SRG, Var, Wkg IT-Col, DE-Hai, ZM-Mon BR-Sa3 US-SRM, Ton		0.80 0.54 0.61	
(Hu & Lei, 2021)	CRO (wheat) CRO (maize)	Weishan, North China Plain	GS mean	0.59 0.44	Values and dynamics of T/ET compared poorly to the two-stage theory of bare soil E. For maize, similar values as ZH16 and smaller values compared to SB17, SK10, and TEA18. Wheat LI19 estimates were greater than PP18, ZH16, and SK10 and smaller than SB17 and TEA18
(Ohkubo et al., 2023)	WET	Kalimantan, Indonesia	Annual mean	0.56	Drained and slightly drained swamps had higher T/ET than the burned degraded swamp (0.21)
(Scott et al., 2021)	DBF GRA	US-CMW US-Wkg	Annual mean	0.36 0.78	Lowest DBF values in the spring/fall compared to ZH16, TEA18, and SB17
(Nie et al., 2021)	DBF EBF ENF MF Misc.	11 sites 3 sites 19 sites 3 sites All (36) forest sites	Annual mean	0.73	
(Wang et al., 2026)	Misc.	368 global EC sites	Annual mean	0.61	Greater values than ZH16, lower values than TEA18
(Maes et al., 2020)	Misc.	86 global FLUXNET sites	Annual mean	0.66	Lower than an LAI-based method (Wei et al., 2017) which showed an inter-site mean of 0.69
(Restrepo-Coupe et al., 2023)	DBF	Tapajos national forest, Brazil	From daily T and E totals	0.86	Seasonal trends correlated with incoming shortwave radiation and LAI. Drought decreased T/ET while a wet La Niña period increased estimates

6.3 PP18

Table A3: Studies that have used the conductance partitioning model by Perez-Preigo et al. (2018) to calculate the transpiration to evapotranspiration ratio (T/ET). The timescales used in the T/ET calculations are listed as well as any comparisons to other ET partitioning methods. Locations are listed by FLUXNET site IDs when applicable, for any non-FLUXNET sites, the location is listed in accordance to how it was reported in the methods of each study. The plant functional types (PFT) of the ecosystems are identified with CRO: cropland, GRA: grassland, DBF: deciduous broadleaf forest, ENF: evergreen needleleaf forest, EBF: evergreen broadleaf forest, MF: mixed forest, SAV: savanna, WSA: woody savanna, OSH: shrubland, BSV: bare sparse vegetation, WET: wetland. GS: growing season, LAI: leaf area index, HRB: Heihe River Basin. Methods: ZH16: Zhou et al. (2016), LI19: Li et al. (2019), PP18: Perez-Preigo et al. (2018), TEA18: Nelson et al. (2018), SK10: Scanlon & Kustas (2010), SB17: Scott & Biederman (2017).

Reference	PFT	Location	Calculation	T/ET	Notes
(Perez-Priego et al., 2018)	SAV	ES-LMa	GS range	0.20-0.40	Diurnal trends are consistently lower than those from SK10
(Nelson et al., 2020)	Misc.	251 FLUXNET sites	Annual mean	0.45	Similar, slightly lower than T/ET estimates from ZH16 method, lower than TEA18 estimates
(Hu & Lei, 2021)	CRO (wheat)	Weishan, North China Plain	GS mean	0.46	Lower T/ET values and different 14-day trends than the two-stage theory of bare soil evaporation, lower estimates than SB17, SK10, LI19, ZH16, and TEA18
(Liu et al., 2022a)	CRO (maize)	HRB, Daman	GS mean		Lowest T/ET values compared to estimates made with ZH16, TEA18, isotope-based, LAI-based, and remote sensing trapezoid based methods
(Lowry et al., 2021)	WET (native) WET (swamp) ENF	Bribie Island, Queensland, Australia	Annual mean	0.34 0.23 0.55	
(Reich et al., 2024)	WSA	US-Mpj	GS mean	0.60	Higher T/ET estimate than sap-flow but lower than SB17b

6.4 TEA18

Table A4: Studies that have used the Transpiration Estimation Algorithm by Nelson et al. (2018) to calculate the transpiration to evapotranspiration ratio (T/ET). The timescales used in the T/ET calculations are listed as well as any comparisons to other ET partitioning methods. Locations are listed by FLUXNET site IDs when applicable, for any non-FLUXNET sites, the location is listed in accordance to how it was reported in the methods of each study. The plant functional types (PFT) of the ecosystems are identified with CRO: cropland, GRA: grassland, DBF: deciduous broadleaf forest, ENF: evergreen needleleaf forest, EBF: evergreen broadleaf forest, MF: mixed forest, SAV: savanna, WSA: woody savanna, OSH: shrubland, BSV: bare sparse vegetation, WET: wetland. GS: growing season, LAI: leaf area index, HRB: Heihe River Basin, TSEB: two source energy balance model, TSEB-SM: TSEB aided by soil moisture. Methods: ZH16: Zhou et al. (2016), LI19: Li et al. (2019), PP18: Perez-Preigo et al. (2018), TEA18: Nelson et al. (2018), SK10: Scanlon & Kustas (2010), SB17: Scott & Biederman (2017).

Reference	PFT	Location	Calculation	T/ET	Notes
(Nelson et al., 2018)	DBF	FR-Hes	GS mean	0.77	T/ET estimates agree well with values from the sap flow method. When applied in 2 ENF sites (DE-Tha and FI-Hyy), TEA18 estimates fall within the range of T values predicted from 3 ecosystem models
(D'Acunha et al., 2024)	CRO (soybean) DBF	Amazon agriculture, Cerrado agriculture Lucas do Rio Verde, Cerrado agriculture Jaciara	From annual T, ET totals	0.61 0.60	Higher T/ET estimates than with ZH16

	GRA WSA Misc.	Amazon forest Tanguro, Amazon forest Sinop, Pantanal forest Amazon pasture, Pantanal pasture Cerrado Campo sujo All Mato Grosso, Brazil sites (from above)	Annual mean	0.67 0.71 0.63	
(Nelson et al., 2020)	DBF GRA ENF Misc.	251 FLUXNET sites	Annual mean Peak seasonal	0.70 0.67 0.62 0.77 0.83	Higher T/ET estimates than with ZH16 and PP18
(Hu & Lei, 2021)	CRO (wheat) CRO (maize)	Weishan, North China Plain	GS mean	0.77 0.71	T/ET values and trends agreed well with the two-stage theory of bare soil evaporation, higher estimates than SB17, SK10, LI19, ZH16, and PP18 (for wheat)
(Paul-Limoges et al., 2022)	CRO (wheat) CRO (barley)	CH-Oe2 CH-Oe2	GS mean	0.73 0.75	Increased diurnal and seasonal T/ET trends and values than ZH16 method
(Li et al., 2024e)	ENF	CA-Ca3	Annual mean	0.69	Similar T/ET trends and values to EE22 method, consistently higher than ZH16 estimates
(Liu et al., 2022a)	CRO (maize)	HRB, Daman	GS mean	>0.85	Higher T/ET values than estimates made with ZH16, PP18, isotope-based, LAI-based, and remote sensing trapezoid based methods
(Räsänen et al., 2022)	SAV	Welgegund Research Station, South Africa	GS mean	0.61	Daily T/ET values and seasonal trends consistently higher than with ZH16 and BH16
(Raghav et al., 2022)	CRO (wheat)	GRL-FLUXNET sites 1, 2, and 3	GS mean	0.76	Similar, slightly higher T/ET estimates than with SK10, higher estimates than ZH16 method
(Scott et al., 2021)	DBF GRA	US-CMW US-Wkg	Annual mean	0.74 0.46	Similar T/ET values to SB17 with higher estimates than ZH16 and LI19 methods
(Wang et al., 2022)	CRO (rubber) DBF	Northern rubber: Chachoengsao Province, TH Southern rubber: Nakhon Si Thammarat Province, TH Ratchaburi Province, TH	Annual mean	0.78 0.72	
(Xue et al., 2023)	CRO EBF ENF DBF GRA MF OSH SAV	10 sites 6 sites 13 sites 9 sites 11 sites 1 site 2 sites 2 sites	Annual mean	0.33 0.78 0.74 0.70 0.75 0.51 0.34 0.76	Across all ecosystems, T/ET from TEA18 and TSEB-SM were higher than when estimated from ZH16 and TSEB

	WSA Misc.	3 sites All (57 sites)		0.67 0.61	
(Kibler et al., 2023)	DBF WSA	US-CMW US-SRM	GS median	0.87 - 0.92 0.72 - 0.80	
(El-Madany et al., 2021)	SAV	ES-LMa, LM1, LM2	From annual T, ET totals	0.69	Higher T/ET in SAV fertilized with nitrogen (0.70) and SAV fertilized with nitrogen and phosphorus (0.71) than control SAV (0.65)
(Zhang et al., 2025a)	CRO (misc.)	US-ARM, CRT, Twt, Tw2, Tw3 IT-BCi, CA2 DE-Seh, RuS, Kli, Geb FR-Gri, FI-Jok, DK-Fou, CH-Oe2, BE-Lon	GS mean	0.66	Higher than ZH16 values (0.48). Both methods estimated the highest values from maize while ZH16 estimated the lowest values from rapeseed and TEA18 from paddy rice
(Bastos Campos et al., 2025)	CRO (vineyard)	Kaltern-Caldaro, South Tyrol, Northern Italy	GS mean	0.78	Similar but slightly higher estimates than with sap flow measurements
(Liu et al., 2025)	OSH	Yanchi Research Station, Beijing, China	Annual mean	0.59	TEA18 estimates compared well with sap flow measurements. EE22 estimates were ~20% lower than TEA18
(Wang et al., 2026)	Misc.	368 global EC sites	Annual mean	0.63	Higher estimates than compared to ZH16, LI19, and sap flow measurements
(Yang et al., 2025a)	CRO (maize, wheat)	Weishan, North China Plain	GS trend		T dominated ET during the GS. TEA18 estimates agreed well with an ecohydrological model (Weishan model)
(Hao et al., 2024)	ENF	CA-LP1	Annual trend		Consistently higher than ZH16 estimates although both methods had similar trends
(Zheng et al., 2024)	CRO (wheat)	Zhao Xian, Shijiazhuang City, Hebei Province, China	Annual trend		Similar estimates to ZH16
(Yu et al., 2022)	CRO DBF EBF ENF GRA WSA	DE-RuS, Seh, US-CRT, Ne1, Ne2, Ne3 CA-Oas, DE-Hai, FR-Fon, US-Ha1, UMB FR-Pue, IT-Cpz CA-NS3, DE-Obe, NL-Loo, US-NR1 DE-Gri, US-Arb, Arc, Goo, SRG US-SRM, Ton	Annual trend		Similar trends when compared to an EC/LSM-based method across global PFTs and ZH16

6.5 SK10

Table A5: Studies that have used the Flux Variance Similarity partitioning method by Scanlon & Kustas (2010) to calculate the transpiration to evapotranspiration ratio (T/ET). The timescales used in the T/ET calculations are listed as well as any comparisons to other ET partitioning methods. Locations are listed by FLUXNET site IDs when applicable, for any non-

FLUXNET sites, the location is listed in accordance to how it was reported in the methods of each study. The plant functional types (PFT) of the ecosystems are identified with CRO: cropland, GRA: grassland, DBF: deciduous broadleaf forest, ENF: evergreen needleleaf forest, EBF: evergreen broadleaf forest, MF: mixed forest, SAV: savanna, WSA: woody savanna, OSH: shrubland, BSV: bare sparse vegetation, WET: wetland. GS: growing season, LAI: leaf area index, HRB: Heihe River Basin, TSEB: two source energy balance model, LSM: land surface model. Methods: ZH16: Zhou et al. (2016), LI19: Li et al. (2019), PP18: Perez-Preigo et al. (2018), TEA18: Nelson et al. (2018), SK10: Scanlon & Kustas (2010), SB17: Scott & Biederman (2017).

Reference	PFT	Location	Calculation	T/ET	Notes
(Hu & Lei, 2021)	CRO (wheat) CRO (maize)	Weishan, North China Plain	GS mean / const ppm	0.55 0.70	T/ET values agreed with values from the two-stage theory of bare soil E and TEA18 for maize, but underestimated wheat comparatively. Values for maize estimations were greater than ZH16, LI19, and SB17 methods and greater than PP18 and ZH16 for wheat.
(Raghav et al., 2022)	CRO (wheat)	GRL-FLUXNET sites 1, 2, and 3	GS mean / const ratio	0.75	Similar T/ET estimates with TEA18 method, higher estimates than ZH16 method
(Wang et al., 2016a)	GRA	Xilin River watershed, Inner Mongolia, China	GS mean / const ppm	0.65	Winter grazing and heavy grazing saw lower T/ET than ungrazed treatments
(Schreiner-McGraw et al., 2022)	CRO (pistachio) CRO (almond)	US-PSL, PSH US-ASL, ASM, ASH	Annual mean / const ppm	0.79 0.65	
(De Haan et al., 2021)	CRO (alfalfa) CRO (maize)	Hopewell Creek Watershed, Ontario, Canada	GS mean / const ppm	0.58 0.71	Alfalfa T/ET showed less seasonality than the maize
(Gao et al., 2024)	CRO (wheat)	Zhangye Oasis, Gansu Province, China	GS mean / const ratio	0.55	
(Ferrara et al., 2024)	CRO (watermelon)	CREA-AA Research Unit, Italy	From GS T, E totals / const ppm	0.51	
(Rana et al., 2018)	CRO (fava bean) CRO (wheat)	CREA-AA Research Unit, Italy	Emergence stage (flowering stage) / const ppm	0.25 (0.43) 0.30 (0.37)	
(Anupoju et al., 2024)	CRO (rice)	Vizianagaram, Andhra Pradesh, India	GS mean / const ppm	0.70	Similar T/ET values as FAO Dual Kc-ETo and Priestley-Taylor methods
(Scanlon et al., 2019; Sulman et al., 2016)*	DBF	US-MMS	GS mean / optimum	0.82	Compared to 0.84 during a severe drought year. Similar T trends with slightly lower values as a sub-canopy based method *Sulman et al. (2016) removed low-frequency data using wavelet analysis while Scanlon et al. (2019) used a moving mean window. Both studies used the

					same data and came to a similar conclusion regarding T/ET estimates
(Peddinti & Kambhammettu, 2019)	CRO (citrus orchard)	Goregone village, Vidarbha, India	Annual mean / const ppm	0.66	Similar T/ET from SIMDualKc model
(Wagle et al., 2021a)	CRO (canola)	Grazinglands Research Laboratory, USDA-ARS	GS mean / const ratio	~0.70	No significant difference in T/ET between till and no-till fields
(Wagle et al., 2021b)	CRO (canola) CRO (wheat) CRO (soybean) CRO (maize) CRO (sorghum)	Grazinglands Research Laboratory, USDA-ARS	Peak growth mean / const ppm, const ratio, optimum, linear, sqrt	0.76-0.88 0.75-0.88 0.80-0.86 0.78-0.90 0.66-0.88	Range dependent on which WUE algorithm was used. Const_ppm, const_ratio, and optimum models were consistent with each other and there was a higher T/ET for linear and sqrt models in wheat and canola
(Shveytser et al., 2022)	DBF ENF WET Misc.	US-PFk, PFL, PFm, PFn, PFc, PFp, PFq, PFs, PFi, PFj US-PFb, PFg, PFh, PFt US-PFd, PFe, PFr All sites	GS mean / const ratio	0.54 0.53 0.46 0.52	
(Wagle et al., 2020)	CRO (alfalfa)	Grazinglands Research Laboratory, USDA-ARS	GS mean / const ratio	~0.80	
(Wagle et al., 2023)	CRO (wheat) CRO (canola)	Grazinglands Research Laboratory, USDA-ARS	GS mean / const ppm, const ratio, linear, sqrt, optimum	0.64-0.89 0.59-0.85	Range dependent on WUE algorithm used
(Liu et al., 2022b)	GRA	Bange, Tibetan Plateau	Annual mean / const ratio	0.34	
(Anderson et al., 2018)	CRO (peach orchard)	San Joaquin Valley, California, USA	GS mean / const ppm, const ratio, linear, sqrt	0.48-0.84	Range dependent on WUE algorithm used
(Wang et al., 2016b)	GRA/URB	Broadmead site, New Jersey, USA	Annual mean / const ratio	>0.70	Similar seasonal and diurnal patterns as NOAH LSM but decreased summer T/ET from SK10
(Scanlon & Kustas, 2012)	CRO (corn)	OPE[3], USDA-ARS	Crop maturity / const ratio	0.70-0.80	
(Borges et al., 2024)	DBF	Campina Grande, State of Paraíba, Brazil Serra Negra, State of Rio Grande do Norte, Brazil	Rainy season / const ratio	0.65	Slightly higher T/ET for sparse vegetation cover (0.67) vs. dense vegetation cover (0.64)
(Li et al., 2024b)	DBF/URB	Nankai University, Tianjin, China	GS mean / const ppm, const ratio, sqrt,	0.80-0.88	Range dependent on WUE algorithm used, similar seasonal trends for const ppm, const ratio, sqrt, and optimum. Linear algorithm had higher T/ET values

			optimum, linear		
(Klosterhalfen et al., 2019b)	CRO (wheat) ENF	DE-Rus DE-RuW	Annual median / const ppm	0.77-0.91 0.84	
(Kustas et al., 2018)	CRO (vineyard)	Borden Ranch, California, USA	June mean	0.83	Compared to sap-flow measurements of 0.80
(Wang et al., 2024b)	CRO (poplar plantation)	MinQuan site, Henan Province, China	July, Aug, Sep mean / optimum	0.67	Lower T/ET estimates than TH08 (0.78) method, and higher than the ZN22 (0.63) method
(Gao et al., 2025)	CRO (wheat)	HRB, Zhangye	GS mean / const ratio	0.55	E dominated when looking at annual means
(Wang et al., 2025)	CRO (evergreen plantation) CRO (deciduous plantation)	Jiyuan (JY2) Jinzhai Jianping (JP1, JP2) MinQuan Jiyuan (JY1) Henan Province, China	GS mean, all sites: Const ppm Const ratio Linear Sqrt Optimum	 0.63 0.64 0.78 0.70 0.65	Deciduous plantations had more consistent T/ET values across model runs compared to the evergreen plantation
(Paciolla et al., 2025)	CRO (vineyard)	California, USA	Mean midday peaks, const ratio	~0.60	Much lower than estimates from ZN22, TH08 (midday peaks ~100%). FEST-2-EWB (a two-source LSM) agreed well with ZN22 and TH08 while TSEB produced the highest estimates from all methods
(Scanlon & Kustas, 2010)	CRO (maize)	Maryland, USA	Annual trend		SK10 was able to identify changes in T/ET after precipitation and T estimates followed LAI trends
(Skaggs et al., 2018)	CRO (peach)	San Joaquin Valley, California, USA	GS trend		T/ET decreased under well-watered conditions
(Deb Burman et al., 2022)	WET DBF	Tamil Nadu, India Assam, northeast India	Annual trend		WET had higher T/ET during the GS but did not show seasonal dynamics. The DBF had higher T/ET from September to December and showed seasonal variability
(Shih et al., 2025)	EBF ENF	Lien-Hua-Chih, Taiwan Chi-Lan, Taiwan	Daily trend		Higher midday peak T/ET in the EBF with peak values occurring between 12-2pm (local time) while the ENF peaked early and values decreased from 6am-3pm
(Carneiro et al., 2025)	OSH	Dense caatinga Sparse caatinga Northeastern Brazil	Annual mean		Sparse caatinga with more exposed rocky outcrops and bare soil had lower T/ET than the dense caatinga
(Klosterhalfen et al., 2019a)	ENF DBF CRO GRA	4 sites across Europe, 1 site in Oregon, USA 2 sites in Europe 2 sites in Europe 3 sites in Europe	Annual trend		Consistently lower T estimates than TH08 across all ecosystems. SK10 showed no clear difference in T/ET across biomes

(Good et al., 2014)	CRO (pistachio and almond)	Mpala Research Center, Kenya	GS trend		Similar to the isotope method during peak GS, but showed T before any green leaves had sprouted and continued after senescence
(Kustas et al., 2019a)	CRO (vineyard)	California, USA	GS trend		T estimates agreed well with results from the micro-Bowen ratio method
(Rana et al., 2019)	CRO (vineyard)	Mazaro River Basin, Sicily	Annual trend		T estimates were higher than results from sap flow method
(Song et al., 2018)	CRO (maize)	HRB, Daman	GS trend		T/ET values were 10% lower than results from a MODIS-based dual temperature difference model
(Kustas et al., 2019b)	CRO (vineyard)	California, USA	GS trend		Higher peak seasonal values than the TSEB and TSEB-LAI

6.6 SB17

Table A6: Studies that have used the linear regression-based partitioning method by Scott & Biederman (2017) to calculate the transpiration to evapotranspiration ratio (T/ET). The timescales used in the T/ET calculations are listed as well as any comparisons to other ET partitioning methods. Locations are listed by FLUXNET site IDs when applicable, for any non-FLUXNET sites, the location is listed in accordance to how it was reported in the methods of each study. The plant functional types (PFT) of the ecosystems are identified with CRO: cropland, GRA: grassland, DBF: deciduous broadleaf forest, ENF: evergreen needleleaf forest, EBF: evergreen broadleaf forest, MF: mixed forest, SAV: savanna, WSA: woody savanna, OSH: shrubland, BSV: bare sparse vegetation, WET: wetland. GS: growing season, LSM: land surface model. Methods: ZH16: Zhou et al. (2016), LI19: Li et al. (2019), PP18: Perez-Preigo et al. (2018), TEA18: Nelson et al. (2018), SK10: Scanlon & Kustas (2010), SB17: Scott & Biederman (2017).

Reference	**PFT**	**Location**	**Calculation**	**T/ET**	**Notes**
(MacBean et al., 2020; Scott & Biederman, 2017)*	OSH SAV GRA	US-Whs US-SRM US-SRG, Wkg	GS mean	0.44 0.62 0.51	Similar annual T/ET trends with higher values than estimates made with the ZH16 method *Scott and Biederman (2017) was the method establishment while MacBean et al. (2020) compared outputs to an LSM, which showed lower values and different trends to SB17
(Hu & Lei, 2021)	CRO (wheat) CRO (maize)	Weishan, North China Plain	GS mean	0.70 0.64	Greater maize T/ET values than ZH16 and LI19, smaller values than SK10, TEA18, and the two-stage theory of bare soil evaporation. For wheat, greater values than PP18, ZH16, SK10, and LI19 and smaller values than TEA18
(Ma et al., 2020)	SAV GRA	US-Ton US-Var	GS mean	0.74 0.66	Higher T/ET values than ZH16 with regular (95%) and 80% quantile regression

(Scott et al., 2021)	DBF	US-CMW	Annual mean	0.40	Similar values to TEA18 but higher monthly values than ZH16 and LI19
(Sun & Verseghy, 2019)	OSH	US-Whs	Summer mean	0.49	
(Eichelmann et al., 2022)	WET	US-TW1, TW4, MYB, Sne	Annual trend		Lower values than EE22 for wetland sites with increased standing water. EE22 results compared better with leaf-level T measurements

6.7 Methods with limited testing

Table A7: Studies that have used various partitioning methods found from the literature review to calculate the transpiration to evapotranspiration ratio (T/ET). The timescales used in the T/ET calculations are listed as well as any comparisons to other ET partitioning methods. Locations are listed by FLUXNET site IDs when applicable, for any non-FLUXNET sites, the location is listed in accordance to how it was reported in the methods of each study. The plant functional types (PFT) of the ecosystems are identified with CRO: cropland, GRA: grassland, DBF: deciduous broadleaf forest, ENF: evergreen needleleaf forest, EBF: evergreen broadleaf forest, MF: mixed forest, SAV: savanna, WSA: woody savanna, OSH: shrubland, BSV: bare sparse vegetation, WET: wetland. GS: growing season, TSEB: two source energy balance model, LSM: land surface model. Methods: ZH16: Zhou et al. (2016), LI19: Li et al. (2019), PP18: Perez-Preigo et al. (2018), TEA18: Nelson et al. (2018), SK10: Scanlon & Kustas (2010), SB17: Scott & Biederman (2017), BH16: Berkelhammer et al. (2016), TH08: Thomas et al. (2008), ZN22: Zahn et al. (2022), SB17b: Reich et al. (2024), EE22: Eichelmann et al. (2022). Method types: uWUE: underlying water use efficiency, HF: high frequency, LR: linear regression, ML: machine learning.

Method	Method type	Reference	PFT	Location	Calculation	T/ET	Notes
BH16	uWUE	(Berkelhammer et al., 2016)	ENF	US-NR1, MEF	Annual mean	0.56	Trends agree with isotopic approach on the synoptic scale
BH16	uWUE	(Räsänen et al., 2022)	SAV	Welgegund Research Station, South Africa	GS mean	0.46	Daily T/ET values lower than with TEA18 and ZH16 methods
BH16	uWUE	(Dukat et al., 2023)	ENF	Mezyk and Tuczno, Poland	GS mean	0.75	Much higher T/ET estimate than with sap flow method (0.48)
BH16	uWUE	(Knowles et al., 2023)	ENF	US-NR1, GLEES			31% decrease in T relative to ET after a bark beetle pathogen outbreak while T recovered quicker than ET post outbreak
BH16	uWUE	(Cammalleri et al., 2024)	CRO (almond, olive, vineyard)	California, USA			Similar T/ET estimates to various TSEB models (PT, PM, 2T)

TH08 ZN22	HF HF	(Wang et al., 2024b)	CRO (poplar plantation)	MinQuan site, Henan Province, China	July, Aug, Sep mean	0.78 0.63	TH08 estimated value was higher than SK10 (0.67), while ZN22 estimated value was the lowest of the three methods
ZN22	HF	(Zahn et al., 2022)	GRA ENF	Mpala Research Center, Kenya Wind River Experimental forest, USA	Dry period mean Summer mean	0.51 0.62	Similar seasonal trends as TH08, SK10, and the isotopic method
ZN22	HF	(Amaro Medina et al., 2025)	WET	Sandhill Fen, Alberta, Canada	GS mean	~0.70	
SK10/ ZN22/ TH08	HF (all)	(Zahn & Bou-Zeid, 2024)	Misc.	47 NEON sites	Winter mean Summer mean	0.5 0.7	TH08 and ZN22 estimated higher values in the summer when compared to SK10, ZN22b and TH08b
TH08/ ZN22/ SK10	HF (all)	(Paciolla et al., 2025)	CRO (vineyard)	California, USA	Mean midday peaks	~1.0	ZN22 and TH08 had higher estimates than SK10 (midday peaks ~60%). FEST-2-EWB (a two-source LSM) agreed well with ZN22 and TH08 while TSEB produced the highest estimates from all methods
ZH16 & SB17*	uWUE/ LR	(Yuan et al., 2021)	GRA/ WSA	US-SRG / US-SRM	GS mean / uWUE and SB17 methods averaged	0.68	*ZH16 was corrected based on SB17 estimates and results are a combination of methods Maximum T/ET occurred in October (0.84) and minimum occurred in December (0.14). Individual monthly estimates were lower with SB17 than with ZH16.
RB26	HF/ML	(Ranjbar et al., 2026)	CRO DBF GRA MF ENF SAV OSH	35 NEON sites	Annual trends		Peak T/ET in GS, reaching 0.6 Peak in summer with values >0.6 Similar trends to DBF but with lower daily maximums Highest values in summer Stable values throughout the year Highest values in winter Highest values in summer but low values overall

SB17b	LR	(Reich et al., 2024)	GRA OSH SAV WSA ENF	US-Seg US-Ses US-Wjs US-Mpj US-Vcp, Vcm, Vcs	GS mean	0.88 0.84 0.94 0.87 0.93	Low elevation sites (US-Seg, Ses) agreed well with SB17, the mid- and high-elevation sites did not agree with SB17 estimates. WSA values were higher with SB17b than PP18
EE22	ML	(Eichelmann et al., 2022)	WET	US-TW1, TW4, MYP, Sne	Annual trend		T/ET trends agreed well with leaf-level T measurements and followed GEP patterns, estimates were higher than SB17
EE22	ML	(Liu et al., 2025)	OSH	Yanchi Research Station, Beijing, China	Annual mean		Estimates were ~20% lower than TEA18 and sap flow values
EE22	ML	(Li et al., 2024e)	ENF	CA-Ca3	Annual trend		Trends and values agreed well with TEA18, which were both higher than ZH16

Data availability

No datasets were used in this article

Author contributions

EGC and EE were involved in conceptualization, EGC performed the analysis used to create figures and tables and prepared the manuscript. All co-authors contributed to writing.

Competing interests

The authors declare that they have no conflict of interest.

Financial support

The research was funded from a University College Dublin School of Biology and Environmental Science Demonstratorship.

References

A, Y., Wang, G., Hu, P., Wang, L., Xue, B., and Shrestha, S.: Modification and upscaling of S–W model based on vertical distributions of soil moisture and vegetation root biomass, Environ. Res., 208, https://doi.org/10.1016/j.envres.2022.112765, 2022.

Addington, R. N., Mitchell, R. J., Oren, R., and Donovan, L. A.: Stomatal sensitivity to vapor pressure deficit and its relationship to hydraulic conductance in Pinus palustris, Tree Physiol., 24, 561–569, 2004.

Amaro Medina, D., Clark, M. G., and Carey, S. K.: Multi-Year Evapotranspiration and Energy Dynamics of a Reclaimed Fen in the Athabasca Oil Sands Region, Hydrol. Process., 39, https://doi.org/10.1002/hyp.70247, 2025.

Anderson, M., Gao, F., Knipper, K., Hain, C., Dulaney, W., Baldocchi, D., Eichelmann, E., Hemes, K., Yang, Y., Medellin-Azuara, J., and Kustas, W.: Field-scale assessment of land and water use change over the California delta using remote sensing, Remote Sens. (Basel)., 10, https://doi.org/10.3390/rs10060889, 2018.

Anupoju, V., Kambhammettu, B. V. N. P., and Peddinti, S. R.: Comparative analysis of FAO dual Kc, Priestley-Taylor and flux variance similarity methods in partitioning evapotranspiration from flood-irrigated rice fields, Irrigation and Drainage, https://doi.org/10.1002/ird.3039, 2024.

Bai, Y., Li, X., Zhou, S., Yang, X., Yu, K., Wang, M., Liu, S., Wang, P., Wu, X., Wang, X., Zhang, C., Shi, F., Wang, Y., and Wu, Y.: Quantifying plant transpiration and canopy conductance using eddy flux data: An underlying water use efficiency method, Agric. For. Meteorol., 271, 375–384, https://doi.org/10.1016/j.agrformet.2019.02.035, 2019.

Baldocchi, D. D.: Assessing the eddy covariance technique for evaluating carbon dioxide exchange rates of ecosystems: Past, present and future, Glob. Chang. Biol., 9, 479–492, https://doi.org/10.1046/j.1365-2486.2003.00629.x, 2003.

Baldocchi, D. D.: How eddy covariance flux measurements have contributed to our understanding of Global Change Biology, https://doi.org/10.1111/gcb.14807, 1 January 2020.

Bastos Campos, F., Callesen, T. O., Gonzalez, C. V., Alberti, G., Montagnani, L., Tagliavini, M., Nelson, J. A., and Zanotelli, D.: Evapotranspiration Dynamics and Partitioning in a Grassed Vineyard: Ecophysiological and Computational Modeling Approaches, Water Resour. Res., 61, https://doi.org/10.1029/2023WR035360, 2025.

Beer, C., Ciais, P., Reichstein, M., Baldocchi, D., Law, B. E., Papale, D., Soussana, J. F., Ammann, C., Buchmann, N., Frank, D., Gianelle, D., Janssens, I. A., Knohl, A., Köstner, B., Moors, E., Roupsard, O., Verbeeck, H., Vesala, T., Williams, C. A., and Wohlfahrt, G.: Temporal and among-site variability of inherent water use efficiency at the ecosystem level, Global Biogeochem. Cycles, 23, https://doi.org/10.1029/2008GB003233, 2009.

Berkelhammer, M., Noone, D. C., Wong, T. E., Burns, S. P., Knowles, J. F., Kaushik, A., Blanken, P. D., and Williams, M. W.: Convergent approaches to determine an ecosystem's transpiration fraction, Global Biogeochem. Cycles, 30, 933–951, https://doi.org/10.1002/2016GB005392, 2016.

Bishop, C. M.: Neural Networks for Pattern Recognition, Oxford University Press, New York, 1995.

Bonan, G. B., Lawrence, P. J., Oleson, K. W., Levis, S., Jung, M., Reichstein, M., Lawrence, D. M., and Swenson, S. C.: Improving canopy processes in the Community Land Model version 4 (CLM4) using global flux fields empirically inferred from FLUXNET data, J. Geophys. Res., 116, https://doi.org/10.1029/2010jg001593, 2011.

Bonan, G. B., Oleson, K. W., Fisher, R. A., Lasslop, G., and Reichstein, M.: Reconciling leaf physiological traits and canopy flux data: Use of the TRY and FLUXNET databases in the Community Land Model version 4, J. Geophys. Res. Biogeosci., 117, https://doi.org/10.1029/2011JG001913, 2012.

Borges, C. K., Carneiro, R. G., Santos, C. A., Zeri, M., Poczta, P., Cunha, A. P. M. A., Stachlewska, I. S., and dos Santos, C. A. C.: Partitioning of water vapor and CO2 fluxes and underlying water use efficiencyevaluation in a Brazilian seasonally dry tropical forest (Caatinga) using the Fluxpart model, J. South Am. Earth Sci., 142, https://doi.org/10.1016/j.jsames.2024.104963, 2024.

Breiman, L.: Random Forest, Mach. Learn., 45, 5–32, https://doi.org/10.1023/A:1010933404324, 2001.

Brutsaert, W.: Global land surface evaporation trend during the past half century: Corroboration by Clausius-Clapeyron scaling, Adv. Water Resour., 106, 3–5, https://doi.org/10.1016/j.advwatres.2016.08.014, 2017.

Bu, J., Gan, G., Chen, J., Su, Y., García, M., and Gao, Y.: Biophysical constraints on evapotranspiration partitioning for a conductance-based two source energy balance model, J. Hydrol. (Amst)., 603, https://doi.org/10.1016/j.jhydrol.2021.127179, 2021.

Bu, J., Gan, G., Chen, J., Su, Y., Yuan, M., Gao, Y., Domingo, F., López-Ballesteros, A., Migliavacca, M., El-Madany, T. S., Gentine, P., Xiao, J., and Garcia, M.: Dryland evapotranspiration from remote sensing solar-induced chlorophyll fluorescence: Constraining an optimal stomatal model within a two-source energy balance model, Remote Sens. Environ., 303, https://doi.org/10.1016/j.rse.2024.113999, 2024.

Cammalleri, C., Rallo, G., Agnese, C., Ciraolo, G., Minacapilli, M., and Provenzano, G.: Combined use of eddy covariance and sap flow techniques for partition of et fluxes and water stress assessment in an irrigated olive orchard, Agric. Water Manag., 120, 89–97, https://doi.org/10.1016/j.agwat.2012.10.003, 2013.

Cammalleri, C., Anderson, M. C., Bambach, N. E., McElrone, A. J., Knipper, K., Roby, M. C., and Kustas, W. P.: Field scale partitioning of Landsat land surface temperature into soil and canopy components for evapotranspiration assessment using a two-source energy balance model, Irrig. Sci., https://doi.org/10.1007/s00271-024-00976-w, 2024.

Campbell, G. S. and Norman, J. M.: An Introduction to Environmental Biophysics, Springer New York, New York, NY, https://doi.org/10.1007/978-1-4612-1626-1, 1998.

Cao, L., Bala, G., Caldeira, K., Nemani, R., and Ban-Weiss, G.: Importance of carbon dioxide physiological forcing to future climate change, PNAS, 107, 9513–9518, https://doi.org/10.1073/pnas.0913000107/-/DCSupplemental, 2010.

Cao, R., Huang, H., Wu, G., Han, D., Jiang, Z., Di, K., and Hu, Z.: Spatiotemporal variations in the ratio of transpiration to evapotranspiration and its controlling factors across terrestrial biomes, Agric. For. Meteorol., 321, https://doi.org/10.1016/j.agrformet.2022.108984, 2022.

Carneiro, R. G., Rykowska, Z., Borges, C. K., Stachlewska, I. S., and dos Santos, C. A. C.: Energy balance and Evapotranspiration response to environmental variables in the semi-arid Caatinga biome, J. South Am. Earth Sci., 152, https://doi.org/10.1016/j.jsames.2024.105319, 2025.

Chaney, N. W., Herman, J. D., Ek, M. B., and Wood, E. F.: Deriving global parameter estimates for the Noah land surface model using FLUXNET and machine learning, J. Geophys. Res., 121, 13,218-13,235, https://doi.org/10.1002/2016JD024821, 2016.

Chang, X., Feng, Q., and Ning, T.: Quantifying Water Use Efficiency Across Different Ecosystems Based on Eddy-Flux Observations, Hydrol. Process., 39, https://doi.org/10.1002/hyp.70327, 2025.

Chatterjee, S., Swain, C. K., Nayak, A. K., Chatterjee, D., Bhattacharyya, P., Mahapatra, S. S., Debnath, M., Tripathi, R., Guru, P. K., and Dhal, B.: Partitioning of eddy covariance-measured net ecosystem exchange of CO2 in tropical lowland paddy, Paddy and Water Environment, 18, 623–636, https://doi.org/10.1007/s10333-020-00806-7, 2020.

Chen, H., Wei, Y., and Huang, J. J.: Widespread increase in plant transpiration driven by global greening, Glob. Planet. Change, 235, https://doi.org/10.1016/j.gloplacha.2024.104395, 2024.

Chen, Y., Ding, Z., Yu, P., Yang, H., Song, L., Fan, L., Han, X., Ma, M., and Tang, X.: Quantifying the variability in water use efficiency from the canopy to ecosystem scale across main croplands, Agric. Water Manag., 262, https://doi.org/10.1016/j.agwat.2021.107427, 2022.

Chen, Y., Tang, X., Yao, L., Zhao, Y., Li, G., Wu, C., Zhou, Y., and Sharma, A.: Management practices regulate the response of canopy and ecosystem water use efficiency in cropland ecosystems, Field Crops Res., 304, https://doi.org/10.1016/j.fcr.2023.109166, 2023.

Coenders-Gerritis, A. M. J., van der Ent, R. J., Bogaard, T. A., Wang-Erlandsson, L., Hrachowitz, M., and Savenije, H. H. G.: Uncertainties in transpiration estimates, https://doi.org/10.1038/nature12926, 2014.

Cowan, I. R. and Farquhar, G. D.: Stomatal function in relation to leaf metabolism and environment: Stomatal function in the regulation of gas exchange, Symp. Soc. Exp. Biol., 31, 471–505, 1977.

Cui, N., Zheng, S., Jiang, S., Wang, M., Zhao, L., He, Z., Feng, Y., Wang, Y., Gong, D., Liu, C., and Qiu, R.: Evapotranspiration partitioning based on underlying conductance in a complex tree-grass orchard ecosystem in the humid area of southern China, Agric. For. Meteorol., 344, https://doi.org/10.1016/j.agrformet.2023.109796, 2024.

Czikowsky, M. J. and Fitzjarrald, D. R.: Detecting rainfall interception in an Amazonian rain forest with eddy flux measurements, J. Hydrol. (Amst)., 377, 92–105, https://doi.org/10.1016/j.jhydrol.2009.08.002, 2009.

D'Acunha, B., Dalmagro, H. J., Zanella de Arruda, P. H., Biudes, M. S., Lathuillière, M. J., Uribe, M., Couto, E. G., Brando, P. M., Vourlitis, G., and Johnson, M. S.: Changes in evapotranspiration, transpiration and evaporation across natural and managed landscapes in the Amazon, Cerrado and Pantanal biomes, Agric. For. Meteorol., 346, https://doi.org/10.1016/j.agrformet.2023.109875, 2024.

Dawson, T. E., Burgess, S. S. O., Tu, K. P., Oliveira, R. S., Santiago, L. S., Fisher, J. B., Simonin, K. A., and Ambrose, A. R.: Nighttime transpiration in woody plants from contrasting ecosystems, Tree Physiol., 27, 561–575, https://doi.org/10.1093/treephys/27.4.561, 2007.

Day, M. E.: Influence of temperature and leaf-to-air vapor pressure deficit on net photosynthesis and stomatal conductance in red spruce (Picea rubens), Tree Physiol., 20, 57–63, 2000.

Deb Burman, P. K., Chakraborty, S., El-Madany, T. S., Ramasubramanian, R., Gogoi, N., Gnanamoorthy, P., Murkute, C., Nagarajan, R., and Karipot, A.: A comparative study of ecohydrologies of a tropical mangrove and a broadleaf deciduous forest using eddy covariance measurement, Meteorology and Atmospheric Physics, 134, https://doi.org/10.1007/s00703-021-00840-y, 2022.

Di, N., Xi, B., Clothier, B., Wang, Y., Li, G., and Jia, L.: Diurnal and nocturnal transpiration behaviors and their responses to groundwater-table fluctuations and meteorological factors of Populus tomentosa in the North China Plain, For. Ecol. Manage., 448, 445–456, https://doi.org/10.1016/j.foreco.2019.06.009, 2019.

Van Dijk, A. I. J. M., Gash, J. H., Van Gorsel, E., Blanken, P. D., Cescatti, A., Emmel, C., Gielen, B., Harman, I. N., Kiely, G., Merbold, L., Montagnani, L., Moors, E., Sottocornola, M., Varlagin, A., Williams, C. A., and Wohlfahrt, G.: Rainfall interception and the coupled surface water and energy balance, Agric. For. Meteorol., 214–215, 402–415, https://doi.org/10.1016/j.agrformet.2015.09.006, 2015.

Dolman, A. J., Miralles, D. G., and de Jeu, R. A. M.: Fifty years since Monteith's 1965 seminal paper: The emergence of global ecohydrology, https://doi.org/10.1002/eco.1505, 2014.

Dorigo, W., Dietrich, S., Aires, F., Brocca, L., Carter, S., Cretaux, J. F., Dunkerley, D., Enomoto, H., Forsberg, R., Güntner, A., Hegglin, M. I., Hollmann, R., Hurst, D. F., Johannessen, J. A., Kummerow, C., Lee, T., Luojus, K., Looser, U., Miralles, D. G., Pellet, V., Recknagel, T., Vargas, C. R., Schneider, U., Schoeneich, P., Schröder, M., Tapper, N., Vuglinsky, V., Wagner, W., Yu, L., Zappa, L., Zemp, M., and Aich, V.: Closing the water cycle from observations across scales where do we stand?, https://doi.org/10.1175/BAMS-D-19-0316.1, 1 October 2021.

Dukat, P., Ziemblińska, K., Räsänen, M., Vesala, T., Olejnik, J., and Urbaniak, M.: Scots pine responses to drought investigated with eddy covariance and sap flow methods, Eur. J. For. Res., 142, 671–690, https://doi.org/10.1007/s10342-023-01549-w, 2023.

Eichelmann, E., Mantoani, M. C., Chamberlain, S. D., Hemes, K. S., Oikawa, P. Y., Szutu, D., Valach, A., Verfaillie, J., and Baldocchi, D. D.: A novel approach to partitioning evapotranspiration into evaporation and transpiration in flooded ecosystems, Glob. Chang. Biol., 28, 990–1007, https://doi.org/10.1111/gcb.15974, 2022.

El-Madany, T. S., Reichstein, M., Carrara, A., Martín, M. P., Moreno, G., Gonzalez-Cascon, R., Peñuelas, J., Ellsworth, D. S., Burchard-Levine, V., Hammer, T. W., Knauer, J., Kolle, O., Luo, Y., Pacheco-Labrador, J., Nelson, J. A., Perez-Priego, O., Rolo, V., Wutzler, T., and Migliavacca, M.: How Nitrogen and Phosphorus Availability Change Water Use Efficiency in a Mediterranean Savanna Ecosystem, J. Geophys. Res. Biogeosci., 126, https://doi.org/10.1029/2020JG006005, 2021.

Farquhar, G. D. and Sharkey, T. D.: Stomatal Conductance and Photosynthesis, Annu. Rev. Plant Physiol., 33, 317–345, https://doi.org/10.1146/annurev.pp.33.060182.001533, 1982.

Fatichi, S. and Pappas, C.: Constrained variability of modeled T:ET ratio across biomes, Geophys. Res. Lett., 44, 6795–6803, https://doi.org/10.1002/2017GL074041, 2017.

Feldman, A. F., Short Gianotti, D. J., Konings, A. G., McColl, K. A., Akbar, R., Salvucci, G. D., and Entekhabi, D.: Moisture pulse-reserve in the soil-plant continuum observed across biomes, Nat. Plants, 4, 1026–1033, https://doi.org/10.1038/s41477-018-0304-9, 2018.

Ferrara, R. M., Azzolini, A., Ciurlia, A., De Carolis, G., Mastrangelo, M., Minorenti, V., Montaghi, A., Piarulli, M., Ruggieri, S., Vitti, C., Martinelli, N., and Rana, G.: Carbon and Water Balances in a Watermelon Crop Mulched with Biodegradable Films in Mediterranean Conditions at Extended Growth Season Scale, Atmosphere (Basel)., 15, https://doi.org/10.3390/atmos15080945, 2024.

Fischer, S., Queck, R., Bernhofer, C., and Mauder, M.: Quantifying evaporation of intercepted rainfall: a hybrid correction approach for eddy-covariance measurements, Hydrol. Earth Syst. Sci., 30, 965–984, https://doi.org/10.5194/hess-30-965-2026, 2026.

Fisher, J. B., Melton, F., Middleton, E., Hain, C., Anderson, M., Allen, R., McCabe, M. F., Hook, S., Baldocchi, D., Townsend, P. A., Kilic, A., Tu, K., Miralles, D. D., Perret, J., Lagouarde, J. P., Waliser, D., Purdy, A. J., French, A., Schimel, D., Famiglietti, J. S., Stephens, G., and Wood, E. F.: The future of evapotranspiration: Global requirements for ecosystem functioning, carbon and climate feedbacks, agricultural management, and water resources, https://doi.org/10.1002/2016WR020175, 1 April 2017.

Friend, A. D., Arneth, A., Kiang, N. Y., Lomas, M., Ogée, J., Rödenbeck, C., Running, S. W., Santaren, J. D., Sitch, S., Viovy, N., Ian Woodward, F., and Zaehle, S.: FLUXNET and modelling the global carbon cycle, Glob. Chang. Biol., 13, 610–633, https://doi.org/10.1111/j.1365-2486.2006.01223.x, 2007.

Gan, G. and Liu, Y.: Inferring transpiration from evapotranspiration: A transpiration indicator using the Priestley-Taylor coefficient of wet environment, Ecol. Indic., 110, https://doi.org/10.1016/j.ecolind.2019.105853, 2020.

Gao, H., Cai, Q., Shi, X., Shan, S., and Zhuang, H.: Assessment of irrigation efficiency for arid-zone spring wheat production under flood irrigation, Irrig. Sci., https://doi.org/10.1007/s00271-024-00946-2, 2024.

Gao, H., Cai, Q., Shi, X., Shan, S., and Zhuang, H.: Assessment of irrigation efficiency for arid-zone spring wheat production under flood irrigation, Irrig. Sci., 43, 347–362, https://doi.org/10.1007/s00271-024-00946-2, 2025.

Gedney, N., Cox, P. M., Betts, R. A., Boucher, O., Huntingford, C., and Stott, P. A.: Detection of a direct carbon dioxide effect in continental river runoff records, Nature, 439, 835–838, https://doi.org/10.1038/nature04504, 2006.

Gerken, T., Bromley, G. T., and Stoy, P. C.: Surface moistening trends in the Northern North American great plains increase the likelihood of convective initiation, J. Hydrometeorol., 19, 227–244, https://doi.org/10.1175/JHM-D-17-0117.1, 2018.

Gerrits, A. M. J., Pfister, L., and Savenije, H. H. G.: Spatial and temporal variability of canopy and forest floor interception in a beech forest, Hydrol. Process., 24, 3011–3025, https://doi.org/10.1002/hyp.7712, 2010.

Gnanamoorthy, P., Zhao, J., Chakraborty, A., Burman, P. K. D., Chen, Y., Jiao, L., Zhang, J., Liu, Y., Sivaraj, S., Zhang, Y., and Song, Q.: Asynchronous recovery of evaporation and transpiration following extreme snow damage in a subtropical forest, J. Hydrol. Reg. Stud., 55, https://doi.org/10.1016/j.ejrh.2024.101947, 2024.

Good, S. P., Soderberg, K., Guan, K., King, E. G., Scanlon, T. M., and Caylor, K. K.: δ2H isotopic flux partitioning of evapotranspiration over a grass field following a water pulse and subsequent dry down, Water Resour. Res., 50, 1410–1432, https://doi.org/10.1002/2013WR014333, 2014.

Good, S. P., Noone, D., Kurita, N., Benetti, M., and Bowen, G. J.: D/H isotope ratios in the global hydrologic cycle, Geophys. Res. Lett., 42, 5042–5050, https://doi.org/10.1002/2015GL064117, 2015.

Griffis, T. J.: Tracing the flow of carbon dioxide and water vapor between the biosphere and atmosphere: A review of optical isotope techniques and their application, https://doi.org/10.1016/j.agrformet.2013.02.009, 15 June 2013.

Grossiord, C., Buckley, T. N., Cernusak, L. A., Novick, K. A., Poulter, B., Siegwolf, R. T. W., Sperry, J. S., and McDowell, N. G.: Plant responses to rising vapor pressure deficit, New Phytologist, 226, 1550–1566, https://doi.org/10.1111/nph.16485, 2020.

Guo, Y., Zhu, Z., Zhang, Y., Yao, W., Li, Z., and Lv, Y.: Soil Moisture and Vapor Pressure Deficit Affect Ecosystem Water Use Efficiency via Modulating Gross Primary Productivity to Transpiration Ratio in Rainfed Maize in Northeast China, Plants, 15, https://doi.org/10.3390/plants15081190, 2026.

De Haan, K., Khomik, M., Green, A., Helgason, W., Macrae, M. L., Kompanizare, M., and Petrone, R. M.: Assessment of different water use efficiency calculations for dominant forage crops in the great lakes basin, Agriculture (Switzerland), 11, https://doi.org/10.3390/agriculture11080739, 2021.

Han, D., Wang, G., Liu, T., Xue, B. L., Kuczera, G., and Xu, X.: Hydroclimatic response of evapotranspiration partitioning to prolonged droughts in semiarid grassland, J. Hydrol. (Amst)., 563, 766–777, https://doi.org/10.1016/j.jhydrol.2018.06.048, 2018.

Hao, S., Jia, X., Zhao, H., Li, X., Mu, Y., Zha, T., Liu, P., and Bourque, C. P. A.: Evapotranspiration and its partitioning during and following a mountain pine beetle infestation of a lodgepole pine stand in the interior of British Columbia, Canada, Frontiers in Forests and Global Change, 7, https://doi.org/10.3389/ffgc.2024.1352853, 2024.

Hatfield, J. L. and Dold, C.: Water-use efficiency: Advances and challenges in a changing climate, https://doi.org/10.3389/fpls.2019.00103, 19 February 2019.

Hu, H., Chen, L., Liu, H., Khan, M. Y. A., Tie, Q., Zhang, X., and Tian, F.: Comparison of the vegetation effect on ET partitioning based on eddy covariance method at five different sites of Northern China, Remote Sens. (Basel)., 10, https://doi.org/10.3390/rs10111755, 2018.

Hu, X. and Lei, H.: Evapotranspiration partitioning and its interannual variability over a winter wheat-summer maize rotation system in the North China Plain, Agric. For. Meteorol., 310, https://doi.org/10.1016/j.agrformet.2021.108635, 2021.

Hu, X., Ding, X., Huo, Z., Shi, L., Lin, L., and Jiang, Y.: A Two-Step Strategy for Evapotranspiration Partitioning Within Two-Source Model Frameworks, Agronomy, 16, https://doi.org/10.3390/agronomy16050559, 2026.

Jasechko, S., Sharp, Z. D., Gibson, J. J., Birks, S. J., Yi, Y., and Fawcett, P. J.: Terrestrial water fluxes dominated by transpiration, Nature, 496, 347–350, https://doi.org/10.1038/nature11983, 2013.

Jiang, S., Liang, C., Cui, N., Zhao, L., Liu, C., Feng, Y., Hu, X., Gong, D., and Zou, Q.: Water use efficiency and its drivers in four typical agroecosystems based on flux tower measurements, Agric. For. Meteorol., 295, https://doi.org/10.1016/j.agrformet.2020.108200, 2020.

Jin, J., Yan, T., Wang, H., Ma, X., He, M., Wang, Y., Wang, W., Guo, F., Cai, Y., Zhu, Q., and Wu, J.: Improved modeling of canopy transpiration for temperate forests by incorporating a LAI-based dynamic parametrization scheme of stomatal slope, Agric. For. Meteorol., 326, https://doi.org/10.1016/j.agrformet.2022.109157, 2022.

Jocher, G., Marshall, J., Nilsson, M. B., Linder, S., De Simon, G., Hörnlund, T., Lundmark, T., Näsholm, T., Ottosson Löfvenius, M., Tarvainen, L., Wallin, G., and Peichl, M.: Impact of Canopy Decoupling and Subcanopy Advection on the Annual Carbon Balance of a Boreal Scots Pine Forest as Derived From Eddy Covariance, J. Geophys. Res. Biogeosci., 123, 303–325, https://doi.org/10.1002/2017JG003988, 2018.

Jung, M., Reichstein, M., Ciais, P., Seneviratne, S. I., Sheffield, J., Goulden, M. L., Bonan, G., Cescatti, A., Chen, J., De Jeu, R., Dolman, A. J., Eugster, W., Gerten, D., Gianelle, D., Gobron, N., Heinke, J., Kimball, J., Law, B. E., Montagnani, L., Mu, Q., Mueller, B., Oleson, K., Papale, D., Richardson, A. D., Roupsard, O., Running, S., Tomelleri, E., Viovy, N., Weber, U., Williams, C., Wood, E., Zaehle, S., and Zhang, K.: Recent decline in the global land evapotranspiration trend due to limited moisture supply, Nature, 467, 951–954, https://doi.org/10.1038/nature09396, 2010.

Jung, M., Koirala, S., Weber, U., Ichii, K., Gans, F., Camps-Valls, G., Papale, D., Schwalm, C., Tramontana, G., and Reichstein, M.: The FLUXCOM ensemble of global land-atmosphere energy fluxes, Sci. Data, 6, https://doi.org/10.1038/s41597-019-0076-8, 2019.

Katul, G. G., Palmroth, S., and Oren, R.: Leaf stomatal responses to vapour pressure deficit under current and CO_2-enriched atmosphere explained by the economics of gas exchange, Plant Cell Environ., 32, 968–979, https://doi.org/10.1111/j.1365-3040.2009.01977.x, 2009.

Katul, G. G., Oren, R., Manzoni, S., Higgins, C., and Parlange, M. B.: Evapotranspiration: A process driving mass transport and energy exchange in the soil-plant-atmosphere-climate system, https://doi.org/10.1029/2011RG000366, 1 September 2012.

Kibler, C. L., Trugman, A. T., Roberts, D. A., Still, C. J., Scott, R. L., Caylor, K. K., Stella, J. C., and Singer, M. B.: Evapotranspiration regulates leaf temperature and respiration in dryland vegetation, Agric. For. Meteorol., 339, https://doi.org/10.1016/j.agrformet.2023.109560, 2023.

Kim, S. H., Sicher, R. C., Bae, H., Gitz, D. C., Baker, J. T., Timlin, D. J., and Reddy, V. R.: Canopy photosynthesis, evapotranspiration, leaf nitrogen, and transcription profiles of maize in response to CO_2 enrichment, Glob. Chang. Biol., 12, 588–600, https://doi.org/10.1111/j.1365-2486.2006.01110.x, 2006.

Klosterhalfen, A., Moene, A. F., Schmidt, M., Scanlon, T. M., Vereecken, H., and Graf, A.: Sensitivity analysis of a source partitioning method for H_2O and CO_2 fluxes based on high frequency eddy covariance data: Findings from field data and large eddy simulations, Agric. For. Meteorol., 265, 152–170, https://doi.org/10.1016/j.agrformet.2018.11.003, 2019a.

Klosterhalfen, A., Graf, A., Brüggemann, N., Drüe, C., Esser, O., González-Dugo, M. P., Heinemann, G., Jacobs, C. M. J., Mauder, M., Moene, A. F., Ney, P., Pütz, T., Rebmann, C., Rodríguez, M. R., Scanlon, T. M., Schmidt, M., Steinbrecher, R., Thomas, C. K., Valler, V., Zeeman, M. J., and Vereecken, H.: Source partitioning of H2O and CO2 fluxes based on high-frequency eddy covariance data: A comparison between study sites, Biogeosciences, 16, 1111–1132, https://doi.org/10.5194/bg-16-1111-2019, 2019b.

Knowles, J. F., Bjarke, N. R., Badger, A. M., Berkelhammer, M., Biederman, J. A., Blanken, P. D., Bretfeld, M., Burns, S. P., Ewers, B. E., Frank, J. M., Hicke, J. A., Lestak, L., Livneh, B., Reed, D. E., Scott, R. L., and Molotch, N. P.: Bark beetle impacts on forest evapotranspiration and its partitioning, Science of the Total Environment, 880, https://doi.org/10.1016/j.scitotenv.2023.163260, 2023.

Kool, D., Agam, N., Lazarovitch, N., Heitman, J. L., Sauer, T. J., and Ben-Gal, A.: A review of approaches for evapotranspiration partitioning, https://doi.org/10.1016/j.agrformet.2013.09.003, 15 January 2014.

Kurc, S. A. and Small, E. E.: Soil moisture variations and ecosystem-scale fluxes of water and carbon in semiarid grassland and shrubland, Water Resour. Res., 43, https://doi.org/10.1029/2006WR005011, 2007.

Kustas, W. P., Anderson, M. C., Alfieri, J. G., Knipppper, K., Torres-Rua, A., Parry, C. K., Nieto, H., Agam, N., White, W. A., Gao, F., McKee, L., Prueger, J. H., Hipppps, L. E., Los, S., Alsina, M. M., Sanchez, L., Sams, B., Dokoozlian, N., McKee, M., Jones, S., Yang, Y., Wilson, T. G., Lei, F., McElrone, A., Heitman, J. L., Howard, A. M., Post, K., Melton, F., and Hain, C.: The grape remote sensing atmospheric profile and evapotranspiration experiment, Bull. Am. Meteorol. Soc., 99, 1791–1812, https://doi.org/10.1175/BAMS-D-16-0244.1, 2018.

Kustas, W. P., Agam, N., Alfieri, J. G., McKee, L. G., Prueger, J. H., Hipps, L. E., Howard, A. M., and Heitman, J. L.: Below canopy radiation divergence in a vineyard: implications on interrow surface energy balance, Irrig. Sci., 37, 227–237, https://doi.org/10.1007/s00271-018-0601-0, 2019a.

Kustas, W. P., Alfieri, J. G., Nieto, H., Wilson, T. G., Gao, F., and Anderson, M. C.: Utility of the two-source energy balance (TSEB) model in vine and interrow flux partitioning over the growing season, Irrig. Sci., 37, 375–388, https://doi.org/10.1007/s00271-018-0586-8, 2019b.

Lasslop, G., Reichstein, M., Papale, D., Richardson, A. D., Arneth, A., Barr, A., Stoy, P., and Wohlfahrt, G.: Separation of net ecosystem exchange into assimilation and respiration using a light response curve approach: critical issues and global evaluation, Glob. Chang. Biol., 16, 187–208, https://doi.org/10.1111/j.1365-2486.2009.02041.x, 2010.

Li, C., Han, J., Liu, Z., Tu, Z., and Yang, H.: A harmonized global gridded transpiration product based on collocation analysis, Sci. Data, 11, https://doi.org/10.1038/s41597-024-03425-7, 2024a.

Li, H., Chen, H., and Huang, J. J.: Partitioning urban forest evapotranspiration based on integrating eddy covariance of water vapor and carbon dioxide fluxes, Science of the Total Environment, 935, https://doi.org/10.1016/j.scitotenv.2024.173201, 2024b.

Li, J., Yuan, J., Liu, D., Zhao, X., Dong, Y., Zheng, H., Li, Y., and Ding, W.: Inter- and intra-annual variability and climatic responses of ecosystem water use efficiency in a cool-temperate freshwater wetland, Ecol. Indic., 167, https://doi.org/10.1016/j.ecolind.2024.112663, 2024c.

Li, M., Shao, W., Su, Y., Coenders-Gerrits, M., and Jarsjö, J.: Evidence of field-scale shifts in transpiration dynamics following bark beetle infestation: Stomatal conductance responses, Hydrol. Process., 38, https://doi.org/10.1002/hyp.15162, 2024d.

Li, X., Gentine, P., Lin, C., Zhou, S., Sun, Z., Zheng, Y., Liu, J., and Zheng, C.: A simple and objective method to partition evapotranspiration into transpiration and evaporation at eddy-covariance sites, Agric. For. Meteorol., 265, 171–182, https://doi.org/10.1016/j.agrformet.2018.11.017, 2019.

Li, X., Black, T. A., Zha, T., Jassal, R. S., Nesic, Z., Lee, S. C., Bourque, C. P. A., Hao, S., Jin, C., Liu, P., Jia, X., and Tian, Y.: Long-term trend and interannual variation in evapotranspiration of a young temperate Douglas-fir stand over 2002–2022 reveals the impacts of climate change, Plant Cell Environ., https://doi.org/10.1111/pce.15000, 2024e.

Lian, X., Piao, S., Huntingford, C., Li, Y., Zeng, Z., Wang, X., Ciais, P., McVicar, T. R., Peng, S., Ottlé, C., Yang, H., Yang, Y., Zhang, Y., and Wang, T.: Partitioning global land evapotranspiration using CMIP5 models constrained by observations, Nat. Clim. Chang., 8, 640–646, https://doi.org/10.1038/s41558-018-0207-9, 2018.

Lian, X., Zhao, W., and Gentine, P.: Recent global decline in rainfall interception loss due to altered rainfall regimes, Nat. Commun., 13, https://doi.org/10.1038/s41467-022-35414-y, 2022.

Lin, C., Gentine, P., Huang, Y., Guan, K., Kimm, H., and Zhou, S.: Diel ecosystem conductance response to vapor pressure deficit is suboptimal and independent of soil moisture, Agric. For. Meteorol., 250–251, 24–34, https://doi.org/10.1016/j.agrformet.2017.12.078, 2018.

Liu, B., Hou, J., Ge, H., Liu, M., Shi, L., Li, C., and Cui, Y.: Comparison of Evapotranspiration Partitioning and Dual Crop Coefficients of Direct-Seeded and Transplanted Rice in the Poyang Lake Basin, China, Agronomy, 13, https://doi.org/10.3390/agronomy13051218, 2023.

Liu, M., Tang, R., Li, Z. L., Duan, S., Gao, M., Xu, Z., and Song, L.: Separating soil evaporation from vegetation transpiration by remotely sensed one-phase and two-phase trapezoids, Agric. For. Meteorol., 327, https://doi.org/10.1016/j.agrformet.2022.109215, 2022a.

Liu, P., Zha, T., Jia, X., Tian, Y., Hao, S., and Li, X.: Divergent responses of canopy and ecosystem water use efficiency to environmental conditions over a decade in a shrubland ecosystem dominated by Artemisia ordosica, Agric. For. Meteorol., 368, https://doi.org/10.1016/j.agrformet.2025.110551, 2025.

Liu, Y. and Qiao, C.: Partitioning Evapotranspiration in a Cotton Field under Mulched Drip Irrigation Based on the Water-Carbon Fluxes Coupling in an Arid Region in Northwestern China, Agriculture (Switzerland), 13, https://doi.org/10.3390/agriculture13061219, 2023.

Liu, Y., Zhang, Y., Shan, N., Zhang, Z., and Wei, Z.: Global assessment of partitioning transpiration from evapotranspiration based on satellite solar-induced chlorophyll fluorescence data, J. Hydrol. (Amst)., 612, https://doi.org/10.1016/j.jhydrol.2022.128044, 2022b.

Liu, Y., Liu, H., Li, F., Du, Q., Xu, L., and Li, Y.: Interannual Variations of Water and Carbon Dioxide Fluxes over a Semiarid Alpine Steppe on the Tibetan Plateau, Advances in Meteorology, 2022, https://doi.org/10.1155/2022/7368882, 2022c.

López, J., Way, D. A., and Sadok, W.: Systemic effects of rising atmospheric vapor pressure deficit on plant physiology and productivity, https://doi.org/10.1111/gcb.15548, 1 May 2021a.

López, J. R., Schoppach, R., and Sadok, W.: Harnessing nighttime transpiration dynamics for drought tolerance in grasses, Plant Signal. Behav., 16, 1875646, https://doi.org/10.1080/15592324.2021.1875646, 2021b.

Lowry, A. L., McGowan, H. A., and Gray, M. A.: Multi-year carbon and water exchanges over contrasting ecosystems on a sub-tropical sand island, Agric. For. Meteorol., 304–305, https://doi.org/10.1016/j.agrformet.2021.108404, 2021.

Lu, L., Zhang, D., Zhang, J., Zhang, J., Zhang, S., Bai, Y., and Yang, S.: Ecosystem Evapotranspiration Partitioning and Its Spatial–Temporal Variation Based on Eddy Covariance Observation and Machine Learning Method, Remote Sens. (Basel)., 15, https://doi.org/10.3390/rs15194831, 2023.

Ma, L., Chen, Z., Hao, T., Yang, M., Lin, Q., Zhang, W., Han, L., Liu, Z., Sun, M., Lin, Y., Zhu, X., Chen, S., Dong, G., Gao, Y., Hao, Y., Jiang, S., Niu, S., Shi, P., Tan, J., Tang, Y., Zhang, F., Zhang, Y., Zhao, L., Zhou, L., and Yu, G.: Spatial patterns and environmental drivers of evapotranspiration across the Chinese Grassland Transect, J. Hydrol. (Amst)., 667, 134920, https://doi.org/10.1016/j.jhydrol.2026.134920, 2026.

Ma, S., Eichelmann, E., Wolf, S., Rey-Sanchez, C., and Baldocchi, D. D.: Transpiration and evaporation in a Californian oak-grass savanna: Field measurements and partitioning model results, Agric. For. Meteorol., 295, https://doi.org/10.1016/j.agrformet.2020.108204, 2020.

MacBean, N., Scott, R. L., Biederman, J. A., Ottlé, C., Vuichard, N., Ducharne, A., Kolb, T., Dore, S., Litvak, M., and Moore, D. J. P.: Testing water fluxes and storage from two hydrology configurations within the ORCHIDEE land surface model across US semi-arid sites, Hydrol. Earth Syst. Sci., 24, 5203–5230, https://doi.org/10.5194/hess-24-5203-2020, 2020.

Maes, W. H., Pagán, B. R., Martens, B., Gentine, P., Guanter, L., Steppe, K., Verhoest, N. E. C., Dorigo, W., Li, X., Xiao, J., and Miralles, D. G.: Sun-induced fluorescence closely linked to ecosystem transpiration as evidenced by satellite data and radiative transfer models, Remote Sens. Environ., 249, https://doi.org/10.1016/j.rse.2020.112030, 2020.

Maxwell, R. M. and Condon, L. E.: Connections between groundwater flow and transpiration partitioning, Science (1979)., 353, 377–380, https://doi.org/10.1126/science.aaf7891, 2016.

Medlyn, B. E., De Kauwe, M. G., Lin, Y. S., Knauer, J., Duursma, R. A., Williams, C. A., Arneth, A., Clement, R., Isaac, P., Limousin, J. M., Linderson, M. L., Meir, P., Martin-Stpaul, N., and Wingate, L.: How do leaf and ecosystem measures of water-use efficiency compare?, New Phytologist, 216, 758–770, https://doi.org/10.1111/nph.14626, 2017.

Miralles, D. G., Gash, J. H., Holmes, T. R. H., De Jeu, R. A. M., and Dolman, A. J.: Global canopy interception from satellite observations, Journal of Geophysical Research Atmospheres, 115, https://doi.org/10.1029/2009JD013530, 2010.

Miralles, D. G., De Jeu, R. A. M., Gash, J. H., Holmes, T. R. H., and Dolman, A. J.: Magnitude and variability of land evaporation and its components at the global scale, Hydrol. Earth Syst. Sci., 15, 967–981, https://doi.org/10.5194/hess-15-967-2011, 2011.

Misson, L., Baldocchi, D. D., Black, T. A., Blanken, P. D., Brunet, Y., Curiel Yuste, J., Dorsey, J. R., Falk, M., Granier, A., Irvine, M. R., Jarosz, N., Lamaud, E., Launiainen, S., Law, B. E., Longdoz, B., Loustau, D., McKay, M., Paw U, K. T., Vesala, T., Vickers, D., Wilson, K. B., and Goldstein, A. H.: Partitioning forest carbon fluxes with overstory and understory eddy-covariance measurements: A synthesis based on FLUXNET data, Agric. For. Meteorol., 144, 14–31, https://doi.org/10.1016/j.agrformet.2007.01.006, 2007.

Monteith, J. L.: Evaporation and environment, Symp. Soc. Exp. Biol., 19, 205–234, 1965.

Morison, J. I. L. and Gifford, R. M.: Stomatal Sensitivity to Carbon Dioxide and Humidity, Plant Physiol., 71, 789–796, https://doi.org/10.1104/pp.71.4.789, 1983.

Nelson, J. A., Carvalhais, N., Cuntz, M., Delpierre, N., Knauer, J., Ogée, J., Migliavacca, M., Reichstein, M., and Jung, M.: Coupling Water and Carbon Fluxes to Constrain Estimates of Transpiration: The TEA Algorithm, J. Geophys. Res. Biogeosci., 123, 3617–3632, https://doi.org/10.1029/2018JG004727, 2018.

Nelson, J. A., Pérez-Priego, O., Zhou, S., Poyatos, R., Zhang, Y., Blanken, P. D., Gimeno, T. E., Wohlfahrt, G., Desai, A. R., Gioli, B., Limousin, J. M., Bonal, D., Paul-Limoges, E., Scott, R. L., Varlagin, A., Fuchs, K., Montagnani, L., Wolf, S., Delpierre, N., Berveiller, D., Gharun, M., Belelli Marchesini, L., Gianelle, D., Šigut, L., Mammarella, I., Siebicke, L., Andrew Black, T., Knohl, A., Hörtnagl, L., Magliulo, V., Besnard, S., Weber, U., Carvalhais, N., Migliavacca, M., Reichstein, M., and Jung, M.: Ecosystem transpiration and evaporation: Insights from three water flux partitioning methods across FLUXNET sites, Glob. Chang. Biol., 26, 6916–6930, https://doi.org/10.1111/gcb.15314, 2020.

Nie, C., Huang, Y., Zhang, S., Yang, Y., Zhou, S., Lin, C., and Wang, G.: Effects of soil water content on forest ecosystem water use efficiency through changes in transpiration/evapotranspiration ratio, Agric. For. Meteorol., 308–309, https://doi.org/10.1016/j.agrformet.2021.108605, 2021.

Nogueira, M., Boussetta, S., Balsamo, G., Albergel, C., Trigo, I. F., Johannsen, F., Miralles, D. G., and Dutra, E.: Upgrading Land-Cover and Vegetation Seasonality in the ECMWF Coupled System: Verification With FLUXNET Sites, METEOSAT Satellite Land Surface Temperatures, and ERA5 Atmospheric Reanalysis, Journal of Geophysical Research: Atmospheres, 126, https://doi.org/10.1029/2020JD034163, 2021.

Novick, K. A., Ficklin, D. L., Stoy, P. C., Williams, C. A., Bohrer, G., Oishi, A. C., Papuga, S. A., Blanken, P. D., Noormets, A., Sulman, B. N., Scott, R. L., Wang, L., and Phillips, R. P.: The increasing importance of atmospheric demand for ecosystem water and carbon fluxes, Nat. Clim. Chang., 6, 1023–1027, https://doi.org/10.1038/nclimate3114, 2016.

Ocheltree, T. W., Nippert, J. B., and Prasad, P. V. V.: Stomatal responses to changes in vapor pressure deficit reflect tissue-specific differences in hydraulic conductance, Plant Cell Environ., 37, 132–139, https://doi.org/10.1111/pce.12137, 2014.

Ohkubo, S., Hirano, T., and Kusin, K.: Influence of disturbance on transpiration and evaporation in tropical peat swamp forests, J. Hydrol. (Amst)., 620, https://doi.org/10.1016/j.jhydrol.2023.129523, 2023.

Oishi, A. C., Oren, R., and Stoy, P. C.: Estimating components of forest evapotranspiration: A footprint approach for scaling sap flux measurements, Agric. For. Meteorol., 148, 1719–1732, https://doi.org/10.1016/j.agrformet.2008.06.013, 2008.

Oki, T. and Kanae, S.: Global Hydrological Cycles and World Water Resources, 2006.

Paciolla, N., Corbari, C., Kustas, W. P., Nieto, H., Alfieri, J. G., Zahn, E., Gao, F., Prueger, J. H., Alsina, M. M., Hipps, L. E., McKee, L. G., McElrone, A. J., and Bambach, N.: Two-source energy balance schemes exploiting land surface temperature and soil moisture for continuous vineyard water use estimation, Irrig. Sci., 43, 731–753, https://doi.org/10.1007/s00271-024-00991-x, 2025.

Pagán, B. R., Maes, W. H., Gentine, P., Martens, B., and Miralles, D. G.: Exploring the potential of satellite solar-induced fluorescence to constrain global transpiration estimates, Remote Sens. (Basel)., 11, https://doi.org/10.3390/rs11040413, 2019.

Palatella, L., Rana, G., and Vitale, D.: Towards a Flux-Partitioning Procedure Based on the Direct Use of High-Frequency Eddy-Covariance Data, Boundary. Layer. Meteorol., 153, 327–337, https://doi.org/10.1007/s10546-014-9947-x, 2014.

Papale, D. and Valentini, R.: A new assessment of European forests carbon exchanges by eddy fluxes and artificial neural network spatialization, Glob. Chang. Biol., 9, 525–535, https://doi.org/10.1046/j.1365-2486.2003.00609.x, 2003.

Paschalis, A., Fatichi, S., Pappas, C., and Or, D.: Covariation of vegetation and climate constrains present and future T/ET variability, Environmental Research Letters, 13, https://doi.org/10.1088/1748-9326/aae267, 2018.

Paul-Limoges, E., Wolf, S., Eugster, W., Hörtnagl, L., and Buchmann, N.: Below-canopy contributions to ecosystem CO2 fluxes in a temperate mixed forest in Switzerland, Agric. For. Meteorol., 247, 582–596, https://doi.org/10.1016/j.agrformet.2017.08.011, 2017.

Paul-Limoges, E., Wolf, S., Schneider, F. D., Longo, M., Moorcroft, P., Gharun, M., and Damm, A.: Partitioning evapotranspiration with concurrent eddy covariance measurements in a mixed forest, Agric. For. Meteorol., 280, https://doi.org/10.1016/j.agrformet.2019.107786, 2020.

Paul-Limoges, E., Revill, A., Maier, R., Buchmann, N., and Damm, A.: Insights for the Partitioning of Ecosystem Evaporation and Transpiration in Short-Statured Croplands, J. Geophys. Res. Biogeosci., 127, https://doi.org/10.1029/2021JG006760, 2022.

Peddinti, S. R. and Kambhammettu, B. P.: Dynamics of crop coefficients for citrus orchards of central India using water balance and eddy covariance flux partition techniques, Agric. Water Manag., 212, 68–77, https://doi.org/10.1016/j.agwat.2018.08.027, 2019.

Peng, X., Liu, X., Wang, Y., and Cai, H.: Evapotranspiration Partitioning and Estimation Based on Crop Coefficients of Winter Wheat Cropland in the Guanzhong Plain, China, Agronomy, 13, https://doi.org/10.3390/agronomy13122982, 2023.

Penman, H. L.: Natural evaporation from open water, bare soil and grass, Proc. R. Soc. Lond. A Math. Phys. Sci., 193, 120–145, https://doi.org/10.1098/rspa.1948.0037, 1948.

Perez-Priego, O., Katul, G., Reichstein, M., El-Madany, T. S., Ahrens, B., Carrara, A., Scanlon, T. M., and Migliavacca, M.: Partitioning Eddy Covariance Water Flux Components Using Physiological and Micrometeorological Approaches, J. Geophys. Res. Biogeosci., 123, 3353–3370, https://doi.org/10.1029/2018JG004637, 2018.

Perez-Quezada, J. F., Trejo, D., Lopatin, J., Aguilera, D., Osborne, B., Galleguillos, M., Zattera, L., Celis-Diez, J. L., and Armesto, J. J.: Comparison of carbon and water fluxes and the drivers of ecosystem water use efficiency in a temperate rainforest and a peatland in southern South America, Biogeosciences, 21, 1371–1389, https://doi.org/10.5194/bg-21-1371-2024, 2024.

Poyatos, R., Granda, V., Molowny-Horas, R., Mencuccini, M., Steppe, K., and Martínez-Vilalta, J.: SAPFLUXNET: Towards a global database of sap flow measurements, Tree Physiol., 36, 1449–1455, https://doi.org/10.1093/treephys/tpw110, 2016.

Raghav, P., Wagle, P., Kumar, M., Banerjee, T., and Neel, J. P. S.: Vegetation Index-Based Partitioning of Evapotranspiration Is Deficient in Grazed Systems, Water Resour. Res., 58, https://doi.org/10.1029/2022WR032067, 2022.

Rana, G., Palatella, L., Scanlon, T. M., Martinelli, N., and Ferrara, R. M.: CO2 and H2O flux partitioning in a Mediterranean cropping system, Agric. For. Meteorol., 260–261, 118–130, https://doi.org/10.1016/j.agrformet.2018.06.007, 2018.

Rana, G., De Lorenzi, F., Palatella, L., Martinelli, N., and Ferrara, R. M.: Field scale recalibration of the sap flow thermal dissipation method in a Mediterranean vineyard, Agric. For. Meteorol., 269–270, 169–179, https://doi.org/10.1016/j.agrformet.2019.02.018, 2019.

Ranjbar, S., Zahn, E., Losos, D., Hoffman, S., Shrestha, O., Bou-Zeid, E., and Stoy, P. C.: Partitioning Ecosystem Water Fluxes Into Transpiration, Surface Evaporation, and Canopy-Intercepted Evaporation Using Knowledge-Guided Machine Learning at NEON Sites, J. Geophys. Res. Biogeosci., 131, https://doi.org/10.1029/2025JG009478, 2026.

Räsänen, M., Aurela, M., Vakkari, V., Beukes, J. P., Tuovinen, J. P., Van Zyl, P. G., Josipovic, M., Siebert, S. J., Laurila, T., Kulmala, M., Laakso, L., Rinne, J., Oren, R., and Katul, G.: The effect of rainfall amount and timing on annual transpiration in a grazed savanna grassland, Hydrol. Earth Syst. Sci., 26, 5773–5791, https://doi.org/10.5194/hess-26-5773-2022, 2022.

Reavis, C. W., Reba, M. L., and Runkle, B. R. K.: The effects of alternate wetting and drying irrigation on water use efficiency in Mid-South rice, Agric. For. Meteorol., 353, https://doi.org/10.1016/j.agrformet.2024.110069, 2024.

Reich, E. G., Samuels-Crow, K., Bradford, J. B., Litvak, M., Schlaepfer, D. R., and Ogle, K.: A Semi-Mechanistic Model for Partitioning Evapotranspiration Reveals Transpiration Dominates the Water Flux in Drylands, J. Geophys. Res. Biogeosci., 129, https://doi.org/10.1029/2023JG007914, 2024.

Reichstein, M., Falge, E., Baldocchi, D., Papale, D., Aubinet, M., Berbigier, P., Bernhofer, C., Buchmann, N., Gilmanov, T., Granier, A., Grünwald, T., Havránková, K., Ilvesniemi, H., Janous, D., Knohl, A., Laurila, T., Lohila, A., Loustau, D., Matteucci, G., Meyers, T., Miglietta, F., Ourcival, J. M., Pumpanen, J., Rambal, S., Rotenberg, E., Sanz, M., Tenhunen, J., Seufert, G., Vaccari, F., Vesala, T., Yakir, D., and Valentini, R.: On the separation of net ecosystem exchange into assimilation and ecosystem respiration: Review and improved algorithm, https://doi.org/10.1111/j.1365-2486.2005.001002.x, September 2005.

Restrepo-Coupe, N., O'Donnell Christoffersen, B., Longo, M., Alves, L. F., Campos, K. S., da Araujo, A. C., de Oliveira, R. C., Prohaska, N., da Silva, R., Tapajos, R., Wiedemann, K. T., Wofsy, S. C., and Saleska, S. R.: Asymmetric response of Amazon forest water and energy fluxes to wet and dry hydrological extremes reveals onset of a local drought-induced tipping point, Glob. Chang. Biol., 29, 6077–6092, https://doi.org/10.1111/gcb.16933, 2023.

da Rocha, A. E. Q., Santos, E. A., and Patrignani, A.: Partitioning evapotranspiration in a tallgrass prairie using micrometeorological and water use efficiency approaches under contrasting rainfall regimes, J. Hydrol. (Amst)., 608, https://doi.org/10.1016/j.jhydrol.2022.127624, 2022.

da Rocha, A. E. Q., Santos, E. A., and Owensby, C.: Partitioning evapotranspiration and carbon flux in ungrazed and grazed tallgrass prairie, Agric. Ecosyst. Environ., 343, https://doi.org/10.1016/j.agee.2022.108285, 2023.

Salemi, L. F., Groppo, J. D., Trevisan, R., de Moraes, J. M., de Barros Ferraz, S. F., Villani, J. P., Duarte-Neto, P. J., and Martinelli, L. A.: Land-use change in the Atlantic rainforest region: Consequences for the hydrology of small catchments, J. Hydrol. (Amst)., 499, 100–109, https://doi.org/10.1016/j.jhydrol.2013.06.049, 2013.

Scanlon, T. M. and Kustas, W. P.: Partitioning carbon dioxide and water vapor fluxes using correlation analysis, Agric. For. Meteorol., 150, 89–99, https://doi.org/10.1016/j.agrformet.2009.09.005, 2010.

Scanlon, T. M. and Kustas, W. P.: Partitioning Evapotranspiration Using an Eddy Covariance-Based Technique: Improved Assessment of Soil Moisture and Land–Atmosphere Exchange Dynamics, Vadose Zone Journal, 11, https://doi.org/10.2136/vzj2012.0025, 2012.

Scanlon, T. M. and Sahu, P.: On the correlation structure of water vapor and carbon dioxide in the atmospheric surface layer: A basis for flux partitioning, Water Resour. Res., 44, https://doi.org/10.1029/2008WR006932, 2008.

Scanlon, T. M., Schmidt, D. F., and Skaggs, T. H.: Correlation-based flux partitioning of water vapor and carbon dioxide fluxes: Method simplification and estimation of canopy water use efficiency, Agric. For. Meteorol., 279, https://doi.org/10.1016/j.agrformet.2019.107732, 2019.

Schlesinger, W. H. and Jasechko, S.: Transpiration in the global water cycle, Agric. For. Meteorol., 189–190, 115–117, https://doi.org/10.1016/j.agrformet.2014.01.011, 2014.

Schreiner-McGraw, A. P., Ajami, H., Anderson, R. G., and Wang, D.: Integrating partitioned evapotranspiration data into hydrologic models: Vegetation parameterization and uncertainty quantification of simulated plant water use, Hydrol. Process., 36, https://doi.org/10.1002/hyp.14580, 2022.

Scott, R. L. and Biederman, J. A.: Partitioning evapotranspiration using long-term carbon dioxide and water vapor fluxes, Geophys. Res. Lett., 44, 6833–6840, https://doi.org/10.1002/2017GL074324, 2017.

Scott, R. L., Huxman, T. E., Cable, W. L., and Emmerich, W. E.: Partitioning of evapotranspiration and its relation to carbon dioxide exchange in a Chihuahuan Desert shrubland, Hydrol. Process., 20, 3227–3243, https://doi.org/10.1002/hyp.6329, 2006.

Scott, R. L., Knowles, J. F., Nelson, J. A., Gentine, P., Li, X., Barron-Gafford, G., Bryant, R., and Biederman, J. A.: Water Availability Impacts on Evapotranspiration Partitioning, Agric. For. Meteorol., 297, https://doi.org/10.1016/j.agrformet.2020.108251, 2021.

Shih, C. H., Anderson, R. G., Skaggs, T. H., Juang, J. Y., Chen, Y. Y., Jang, Y. S., Gu, R. Y., Huang, C. Y., and Lo, M. H.: Challenges and limitations of applying the flux variance similarity (FVS) method to partition evapotranspiration in a montane cloud forest, Agric. For. Meteorol., 362, https://doi.org/10.1016/j.agrformet.2025.110391, 2025.

Shuttleworth, W. J. and Wallace, J. S.: Evaporation from sparse crops-an energy combination theory, Quart. I. R. Met. SOC, 111, 839–855, 1985.

Shveytser, V., Stoy, P. C., Butterworth, B. J., Wiesner, S., Skaggs, T., Murphy, B., Wutzler, T., El-Madany, T. S., and Desai, A. R.: Evaporation and transpiration from multiple proximal forests and wetlands, https://doi.org/10.1002/essoar.10511759.1, 5 July 2022.

Siddiq, Z. and Cao, K. F.: Nocturnal transpiration in 18 broadleaf timber species under a tropical seasonal climate, For. Eco1. Manage., 418, 47–54, https://doi.org/10.1016/j.foreco.2017.12.043, 2018.

Sinclair, T. R., Tanner, C. B., and Bennett, J. M.: Water-Use Efficiency in Crop Production, Bioscience, 34, 36–40, https://doi.org/10.2307/1309424, 1984.

Skaggs, T. H., Anderson, R. G., Alfieri, J. G., Scanlon, T. M., and Kustas, W. P.: Fluxpart: Open source software for partitioning carbon dioxide and water vapor fluxes, Agric. For. Meteorol., 253–254, 218–224, https://doi.org/10.1016/j.agrformet.2018.02.019, 2018.

Song, L., Liu, S., Kustas, W. P., Nieto, H., Sun, L., Xu, Z., Skaggs, T. H., Yang, Y., Ma, M., Xu, T., Tang, X., and Li, Q.: Monitoring and validating spatially and temporally continuous daily evaporation and transpiration at river basin scale, Remote Sens. Environ., 219, 72–88, https://doi.org/10.1016/j.rse.2018.10.002, 2018.

Song, L., Bateni, S. M., Xu, Y., Xu, T., He, X., Ki, S. J., Liu, S., Ma, M., and Yang, Y.: Reconstruction of remotely sensed daily evapotranspiration data in cloudy-sky conditions, Agric. Water Manag., 255, https://doi.org/10.1016/j.agwat.2021.107000, 2021.

Song, L., Ding, Z., Kustas, W. P., Xu, Y., Zhao, G., Liu, S., Ma, M., Xue, K., Bai, Y., and Xu, Z.: Applications of a thermal-based two-source energy balance model coupled to surface soil moisture, Remote Sens. Environ., 271, https://doi.org/10.1016/j.rse.2022.112923, 2022.

Song, L., Xu, Y., Liddell, M., Cui, Y., Liu, S., and Xu, P.: Application of a two source energy balance model coupled with satellite based soil moisture and thermal infrared data, ISPRS Journal of Photogrammetry and Remote Sensing, 204, 15–26, https://doi.org/10.1016/j.isprsjprs.2023.08.009, 2023a.

Song, L., Ding, Z., Kustas, W. P., Hua, W., Liu, X., Liu, L., Liu, S., Ma, M., Bai, Y., and Xu, Z.: Applications of a Thermal-Based Two-Source Energy Balance Model Coupling the Sun-Induced Chlorophyll Fluorescence Data, IEEE Geoscience and Remote Sensing Letters, 20, https://doi.org/10.1109/LGRS.2023.3240996, 2023b.

Stapleton, A., Eichelmann, E., and Roantree, M.: A framework for constructing machine learning models with feature set optimisation for evapotranspiration partitioning, Applied Computing and Geosciences, 16, 100105, https://doi.org/10.1016/J.ACAGS.2022.100105, 2022.

Stoy, P. C., Katul, G. G., Siqueira, M. B. S., Juang, J. Y., Novick, K. A., Uebelherr, J. M., and Oren, R.: An evaluation of models for partitioning eddy covariance-measured net ecosystem exchange into photosynthesis and respiration, Agric. For. Meteorol., 141, 2–18, https://doi.org/10.1016/j.agrformet.2006.09.001, 2006.

Stoy, P. C., El-Madany, T. S., Fisher, J. B., Gentine, P., Gerken, T., Good, S. P., Klosterhalfen, A., Liu, S., Miralles, D. G., Perez-Priego, O., Rigden, A. J., Skaggs, T. H., Wohlfahrt, G., Anderson, R. G., Coenders-Gerrits, A. M. J., Jung, M., Maes, W. H., Mammarella, I., Mauder, M., Migliavacca, M., Nelson, J. A., Poyatos, R., Reichstein, M., Scott, R. L., and Wolf, S.: Reviews and syntheses: Turning the challenges of partitioning ecosystem evaporation and transpiration into opportunities, Biogeosciences, 16, 3747–3775, https://doi.org/10.5194/bg-16-3747-2019, 2019.

Sulman, B. N., Roman, D. T., Scanlon, T. M., Wang, L., and Novick, K. A.: Comparing methods for partitioning a decade of carbon dioxide and water vapor fluxes in a temperate forest, Agric. For. Meteorol., 226–227, 229–245, https://doi.org/10.1016/j.agrformet.2016.06.002, 2016.

Sun, J. ying, Sun, X. yang, Hu, Z. yong, and Wang, G. xu: Exploring the influence of environmental factors in partitioning evapotranspiration along an elevation gradient on Mount Gongga, eastern edge of the Qinghai-Tibet Platea, China, J. Mt. Sci., 17, 384–396, https://doi.org/10.1007/s11629-019-5687-1, 2020.

Sun, S. and Verseghy, D.: Introducing water-stressed shrubland into the Canadian Land Surface Scheme, J. Hydrol. (Amst)., 579, https://doi.org/10.1016/j.jhydrol.2019.124157, 2019.

Sun, Z., Zheng, Y., Li, X., Tian, Y., Han, F., Zhong, Y., Liu, J., and Zheng, C.: The Nexus of Water, Ecosystems, and Agriculture in Endorheic River Basins: A System Analysis Based on Integrated Ecohydrological Modeling, Water Resour. Res., 54, 7534–7556, https://doi.org/10.1029/2018WR023364, 2018.

Thomas, C., Martin, J. G., Goeckede, M., Siqueira, M. B., Foken, T., Law, B. E., Loescher, H. W., and Katul, G.: Estimating daytime subcanopy respiration from conditional sampling methods applied to multi-scalar high frequency turbulence time series, Agric. For. Meteorol., 148, 1210–1229, https://doi.org/10.1016/j.agrformet.2008.03.002, 2008.

Thomas, C. K., Martin, J. G., Law, B. E., and Davis, K.: Toward biologically meaningful net carbon exchange estimates for tall, dense canopies: Multi-level eddy covariance observations and canopy coupling regimes in a mature Douglas-fir forest in Oregon, Agric. For. Meteorol., 173, 14–27, https://doi.org/10.1016/j.agrformet.2013.01.001, 2013.

Tong, Y., Wang, P., Li, X. Y., Wang, L., Wu, X., Shi, F., Bai, Y., Li, E., Wang, J., and Wang, Y.: Seasonality of the Transpiration Fraction and Its Controls Across Typical Ecosystems Within the Heihe River Basin, Journal of Geophysical Research: Atmospheres, 124, 1277–1291, https://doi.org/10.1029/2018JD029680, 2019.

Wagle, P., Skaggs, T. H., Gowda, P. H., Northup, B. K., and Neel, J. P. S.: Flux variance similarity-based partitioning of evapotranspiration over a rainfed alfalfa field using high frequency eddy covariance data, Agric. For. Meteorol., 285–286, https://doi.org/10.1016/j.agrformet.2020.107907, 2020.

Wagle, P., Gowda, P. H., Northup, B. K., and Neel, J. P. S.: Ecosystem-level water use efficiency and evapotranspiration partitioning in conventional till and no-till rainfed canola, Agric. Water Manag., 250, https://doi.org/10.1016/j.agwat.2021.106825, 2021a.

Wagle, P., Skaggs, T. H., Gowda, P. H., Northup, B. K., Neel, J. P. S., and Anderson, R. G.: Evaluation of Water Use Efficiency Algorithms for Flux Variance Similarity-Based Evapotranspiration Partitioning in C3 and C4 Grain Crops, Water Resour. Res., 57, https://doi.org/10.1029/2020WR028866, 2021b.

Wagle, P., Raghav, P., Kumar, M., and Gunter, S. A.: Influence of water use efficiency parameterizations on flux variance similarity-based partitioning of evapotranspiration, Agric. For. Meteorol., 328, https://doi.org/10.1016/j.agrformet.2022.109254, 2023.

Wang, H., Prentice, I. C., Keenan, T. F., Davis, T. W., Wright, I. J., Cornwell, W. K., Evans, B. J., and Peng, C.: Towards a universal model for carbon dioxide uptake by plants /704/47 /704/158/851 letter, Nat. Plants, 3, 734–741, https://doi.org/10.1038/s41477-017-0006-8, 2017.

Wang, H., Yang, S., Kalisa, W., Zeng, R., Wang, J., Cao, D., Zhang, S., Zhang, J., and Seka, A. M.: Global Patterns of Ecosystem Transpiration and Carbon–Water Coupling: An Intercomparison of Four Partitioning Models Using Eddy Covariance Data for Sustainable Water Management, Sustainability (Switzerland), 18, https://doi.org/10.3390/su18073245, 2026.

Wang, L., Caylor, K. K., Villegas, J. C., Barron-Gafford, G. A., Breshears, D. D., and Huxman, T. E.: Partitioning evapotranspiration across gradients of woody plant cover: Assessment of a stable isotope technique, Geophys. Res. Lett., 37, https://doi.org/10.1029/2010GL043228, 2010.

Wang, L., Good, S. P., and Caylor, K. K.: Global synthesis of vegetation control on evapotranspiration partitioning, Geophys. Res. Lett., 41, 6753–6757, https://doi.org/10.1002/2014GL061439, 2014.

Wang, L., Liu, H., and Bernhofer, C.: Grazing intensity effects on the partitioning of evapotranspiration in the semiarid typical steppe ecosystems in Inner Mongolia, International Journal of Climatology, 36, 4130–4140, https://doi.org/10.1002/joc.4622, 2016a.

Wang, L., Li, Y., Zhang, X., Chen, K., and Siddique, K. H. M.: Soil water content and vapor pressure deficit affect ecosystem water use efficiency through different pathways, J. Hydrol. (Amst)., 640, https://doi.org/10.1016/j.jhydrol.2024.131732, 2024a.

Wang, W., Smith, J. A., Ramamurthy, P., Baeck, M. L., Bou-Zeid, E., and Scanlon, T. M.: On the correlation of water vapor and CO2: Application to flux partitioning of evapotranspiration, Water Resour. Res., 52, 9452–9469, https://doi.org/10.1002/2015WR018161, 2016b.

Wang, X., Blanken, P. D., Kasemsap, P., Petchprayoon, P., Thaler, P., Nouvellon, Y., Gay, F., Chidthaisong, A., Sanwangsri, M., Chayawat, C., Chantuma, P., Sathornkich, J., Kaewthongrach, R., Satakhun, D., and Phattaralerphong, J.: Carbon and Water Cycling in Two Rubber Plantations and a Natural Forest in Mainland Southeast Asia, J. Geophys. Res. Biogeosci., 127, https://doi.org/10.1029/2022JG006840, 2022.

Wang, X., Zhou, Y., Huang, H., Gao, X., Sun, S., Meng, P., and Zhang, J.: Comparing Four Evapotranspiration Partitioning Methods from Eddy Covariance Considering Turbulent Mixing in a Poplar Plantation, Water (Switzerland), 16, https://doi.org/10.3390/w16111548, 2024b.

Wang, X., Li, Z., Zhou, Y., Wang, Y., Ahmad, S., Hu, M., Sun, S., Huang, H., Zhang, J., and Zhai, L.: Evaluation of water use efficiency model in evapotranspiration partitioning from high-frequency eddy covariance data - a comparison between plantation sites, Agric. For. Meteorol., 372, https://doi.org/10.1016/j.agrformet.2025.110663, 2025.

Wang, Y., Cai, H., Yu, L., Peng, X., Xu, J., and Wang, X.: Evapotranspiration partitioning and crop coefficient of maize in dry semi-humid climate regime, Agric. Water Manag., 236, https://doi.org/10.1016/j.agwat.2020.106164, 2020.

Wang, Y., Anderegg, W. R. L., Venturas, M. D., Trugman, A. T., Yu, K., and Frankenberg, C.: Optimization theory explains nighttime stomatal responses, New Phytologist, 230, 1550–1561, https://doi.org/10.1111/nph.17267, 2021.

Wang-Erlandsson, L., Van Der Ent, R. J., Gordon, L. J., and Savenije, H. H. G.: Contrasting roles of interception and transpiration in the hydrological cycle - Part 1: Temporal characteristics over land, Earth System Dynamics, 5, 441–469, https://doi.org/10.5194/esd-5-441-2014, 2014.

Wei, Z., Yoshimura, K., Okazaki, A., Kim, W., Liu, Z., and Yokoi, M.: Partitioning of evapotranspiration using high-frequency water vapor isotopic measurement over a rice paddy field, Water Resour. Res., 51, 3716–3729, https://doi.org/10.1002/2014WR016737, 2015.

Wei, Z., Yoshimura, K., Wang, L., Miralles, D. G., Jasechko, S., and Lee, X.: Revisiting the contribution of transpiration to global terrestrial evapotranspiration, Geophys. Res. Lett., 44, 2792–2801, https://doi.org/10.1002/2016GL072235, 2017.

Wilcox, B. P., Turnbull, L., Young, M. H., Williams, C. J., Ravi, S., Seyfried, M. S., Bowling, D. R., Scott, R. L., Germino, M. J., Caldwell, T. G., and Wainwright, J.: Invasion of shrublands by exotic grasses: Ecohydrological consequences in cold versus warm deserts, Ecohydrology, 5, 160–173, https://doi.org/10.1002/eco.247, 2012.

Williams, M., Richardson, A. D., Reichstein, M., Stoy, P. C., Peylin, P., Verbeeck, H., Carvalhais, N., Jung, M., Hollinger, D. Y., Kattge, J., Leuning, R., Luo, Y., Tomelleri, E., Trudinger, C. M., and Wang, Y.-P.: Improving land surface models with FLUXNET data, Biogeosciences, 1341–1359 pp., 2009.

Wilson, K. B., Hanson, P. J., Mulholland, P. J., Baldocchi, D. D., and Wullschleger, S. D.: A comparison of methods for determining forest evapotranspiration and its components: sap-flow, soil water budget, eddy covariance and catchment water balance, Agricultural and Forest Meteorology, 153–168 pp., 2001.

Wolf, S., Paul-Limoges, E., Sayler, D., and Kirchner, J. W.: Dynamics of evapotranspiration from concurrent above- and below-canopy flux measurements in a montane Sierra Nevada forest, Agric. For. Meteorol., 346, https://doi.org/10.1016/j.agrformet.2023.109864, 2024.

Wu, Y. and Wang, P.: Decadal Dynamics of Energy Balance and Transpiration Fraction in an Alpine Ecosystem: A Modelling and Observational Study, Ecohydrology, 18, https://doi.org/10.1002/eco.70029, 2025.

Xu, C., Zhu, G., Zhang, Y., and Che, T.: Partitioning of Evapotranspiration and Its Response to Eco-Environmental Factors Over an Alpine Grassland on the Qinghai–Tibetan Plateau Based on the SiB2 Model, Hydrol. Process., 38, https://doi.org/10.1002/hyp.15295, 2024.

Xu, Z., Zhu, Z., Liu, S., Song, L., Wang, X., Zhou, S., Yang, X., and Xu, T.: Evapotranspiration partitioning for multiple ecosystems within a dryland watershed: Seasonal variations and controlling factors, J. Hydrol. (Amst)., 598, https://doi.org/10.1016/j.jhydrol.2021.126483, 2021.

Xu, Z., Man, X., Cai, T., Zhang, S., and Duan, L.: Evaporation dominates growing season evapotranspiration: A case study from a boreal larch forest with synchronized water supply and energy demand in China, For. Ecosyst., 15, https://doi.org/10.1016/j.fecs.2025.100385, 2026.

Xue, B., Wang, G., Xiao, J., Tan, Q., Shrestha, S., Sun, W., and Liu, T.: Global evapotranspiration hiatus explained by vegetation structural and physiological controls, Ecol. Eng., 158, https://doi.org/10.1016/j.ecoleng.2020.106046, 2020.

Xue, K., Song, L., Xu, Y., Liu, S., Zhao, G., Tao, S., Magliulo, E., Manco, A., Liddell, M., Wohlfahrt, G., Varlagin, A., Montagnani, L., Woodgate, W., Loubet, B., and Zhao, L.: Estimating ecosystem evaporation and transpiration using a soil moisture coupled two-source energy balance model across FLUXNET sites, Agric. For. Meteorol., 337, https://doi.org/10.1016/j.agrformet.2023.109513, 2023.

Yang, C., Lei, H., Hu, X., and Liu, M.: Development of an ecohydrological model for coupled simulation of water and carbon fluxes, crop growth, and canopy spectra over croplands, Comput. Electron. Agric., 235, https://doi.org/10.1016/j.compag.2025.110336, 2025a.

Yang, S., Zhang, J., Han, J., Bai, Y., Xun, L., Zhang, S., Cao, D., and Wang, J.: The ratio of transpiration to evapotranspiration dominates ecosystem water use efficiency response to drought, Agric. For. Meteorol., 363, https://doi.org/10.1016/j.agrformet.2025.110423, 2025b.

Yu, L., Zhou, S., Zhao, X., Gao, X., Jiang, K., Zhang, B., Cheng, L., Song, X., and Siddique, K. H. M.: Evapotranspiration Partitioning Based on Leaf and Ecosystem Water Use Efficiency, Water Resour. Res., 58, https://doi.org/10.1029/2021WR030629, 2022.

Yuan, R., Chang, L., and Niu, G.: Annual variations of T/ET in a semi-arid region: Implications of plant water use strategies, J. Hydrol. (Amst)., 603, https://doi.org/10.1016/j.jhydrol.2021.126884, 2021.

Yuan, W., Zheng, Y., Piao, S., Ciais, P., Lombardozzi, D., Wang, Y., Ryu, Y., Chen, G., Dong, W., Hu, Z., Jain, A. K., Jiang, C., Kato, E., Li, S., Lienert, S., Liu, S., Nabel, J. E. M. S., Qin, Z., Quine, T., Sitch, S., Smith, W. K., Wang, F., Wu, C., Xiao, Z., and Yang, S.: Increased atmospheric vapor pressure deficit reduces global vegetation growth, 2019.

Zahn, E. and Bou-Zeid, E.: Observational partitioning of water and CO2 fluxes at National Ecological Observatory Network (NEON) sites: A 5-year dataset of soil and plant components for spatial and temporal analysis, Earth Syst. Sci. Data, 16, 5603–5624, https://doi.org/10.5194/essd-16-5603-2024, 2024.

Zahn, E., Bou-Zeid, E., Good, S. P., Katul, G. G., Thomas, C. K., Ghannam, K., Smith, J. A., Chamecki, M., Dias, N. L., Fuentes, J. D., Alfieri, J. G., Kwon, H., Caylor, K. K., Gao, Z., Soderberg, K., Bambach, N. E., Hipps, L. E., Prueger, J. H., and Kustas, W. P.: Direct partitioning of eddy-covariance water and carbon dioxide fluxes into ground and plant components, Agric. For. Meteorol., 315, https://doi.org/10.1016/j.agrformet.2021.108790, 2022.

Zahn, E., Ghannam, K., Chamecki, M., Moene, A. F., Kustas, W. P., Good, S., and Bou-Zeid, E.: Numerical Investigation of Observational Flux Partitioning Methods for Water Vapor and Carbon Dioxide, J. Geophys. Res. Biogeosci., 129, https://doi.org/10.1029/2024JG008025, 2024.

Zeng, Z., Piao, S., Li, L. Z. X., Wang, T., Ciais, P., Lian, X. U., Yang, Y., Mao, J., Shi, X., and Myneni, R. B.: Impact of Earth Greening on the Terrestrial Water Cycle, https://doi.org/10.1175/JCLI-D-17-0236.s1, 2018.

Zeppel, M., Tissue, D., Taylor, D., MacInnis-Ng, C., and Eamus, D.: Rates of nocturnal transpiration in two evergreen temperate woodland species with differing water-use strategies, Tree Physiol., 30, 988–1000, https://doi.org/10.1093/treephys/tpq053, 2010.

Zhang, J., Yang, S., Wang, J., Zeng, R., Zhang, S., Bai, Y., and Zhang, J.: Evapotranspiration Partitioning for Croplands Based on Eddy Covariance Measurements and Machine Learning Models, Agronomy, 15, https://doi.org/10.3390/agronomy15030512, 2025a.

Zhang, Q., Feng, Q., Su, Y., and Jian, C.: Evapotranspiration Partitioning of the Populus euphratica Forest Ecosystem in the Drylands of Northwestern China, Plants, 14, https://doi.org/10.3390/plants14050680, 2025b.

Zhang, W., Jung, M., Migliavacca, M., Poyatos, R., Miralles, D. G., El-Madany, T. S., Galvagno, M., Carrara, A., Arriga, N., Ibrom, A., Mammarella, I., Papale, D., Cleverly, J. R., Liddell, M., Wohlfahrt, G., Markwitz, C., Mauder, M., Paul-Limoges, E., Schmidt, M., Wolf, S., Brümmer, C., Arain, M. A., Fares, S., Kato, T., Ardö, J., Oechel, W., Hanson, C., Korkiakoski, M., Biraud, S., Steinbrecher, R., Billesbach, D., Montagnani, L., Woodgate, W., Shao, C., Carvalhais, N., Reichstein, M., and Nelson, J. A.: The effect of relative humidity on eddy covariance latent heat flux measurements and its implication for partitioning into transpiration and evaporation, Agric. For. Meteorol., 330, https://doi.org/10.1016/j.agrformet.2022.109305, 2023.

Zheng, C., Wang, S., Chen, J. M., Xiao, J., Chen, J., Zhu, K., and Sun, L.: Modeling transpiration using solar-induced chlorophyll fluorescence and photochemical reflectance index synergistically in a closed-canopy winter wheat ecosystem, Remote Sens. Environ., 302, https://doi.org/10.1016/j.rse.2023.113981, 2024.

Zheng, C., Wang, S., Chen, J. M., Xiao, J., Chen, J., Zhang, Z., and Forzieri, G.: Estimating global transpiration from TROPOMI SIF with angular normalization and separation for sunlit and shaded leaves, Remote Sens. Environ., 319, https://doi.org/10.1016/j.rse.2024.114586, 2025.

Zhong, F., Jiang, S., Van Dijk, A. I. J. M., Ren, L., Schellekens, J., and Miralles, D. G.: Revisiting large-scale interception patterns constrained by a synthesis of global experimental data, Hydrol. Earth Syst. Sci., 26, 5647–5667, https://doi.org/10.5194/hess-26-5647-2022, 2022.

Zhou, S., Yu, B., Huang, Y., and Wang, G.: The effect of vapor pressure deficit on water use efficiency at the subdaily time scale, Geophys. Res. Lett., 41, 5005–5013, https://doi.org/10.1002/2014GL060741, 2014.

Zhou, S., Yu, B., Zhang, Y., Huang, Y., and Wang, G.: Partitioning evapotranspiration based on the concept of underlying water use efficiency, Water Resour. Res., 52, 1160–1175, https://doi.org/10.1002/2015WR017766, 2016.

Zhou, S., Yu, B., Zhang, Y., Huang, Y., and Wang, G.: Water use efficiency and evapotranspiration partitioning for three typical ecosystems in the Heihe River Basin, northwestern China, Agric. For. Meteorol., 253–254, 261–273, https://doi.org/10.1016/j.agrformet.2018.02.002, 2018.

Zwieback, S., Chang, Q., Marsh, P., and Berg, A.: Shrub tundra ecohydrology: Rainfall interception is a major component of the water balance, Environmental Research Letters, 14, https://doi.org/10.1088/1748-9326/ab1049, 2019.